IOP PUBLISHING NONLINEARITY

Nonlinearity **22** (2009) 1337–1366 doi:10.1088/0951-7715/22/6/005

Shock structure in continuum models of gas dynamics: stability and bifurcation analysis

Srboljub S Simić

Department of Mechanics, Faculty of Technical Sciences, University of Novi Sad, Trg Dositeja Obradovića 6, 21000 Novi Sad, Serbia

E-mail: ssimic@uns.ac.rs

Received 25 July 2008, in final form 11 March 2009
Published 24 April 2009
Online at stacks.iop.org/Non/22/1337

Recommended by L Bunimovich

Abstract

The problem of shock structure in gas dynamics is analysed through a comparative study of two continuum models: the parabolic Navier–Stokes–Fourier model and the hyperbolic system of 13 moments equations modeling viscous, heat-conducting monatomic gases within the context of extended thermodynamics. When dissipative phenomena are neglected these models both reduce to classical Euler's equations of gas dynamics. The shock profile solution, assumed in the form of a planar travelling wave, reduces the problem to a system of ordinary differential equations, and equilibrium states appear to be stationary points of the system. It is shown that in both models an upstream equilibrium state suffers an exchange of stability when the shock speed crosses the critical value which coincides with the highest characteristic speed of the Euler's system. At the same time a downstream equilibrium state could be seen as a steady bifurcating solution, while the shock profile represents a heteroclinic orbit connecting the two stationary points. Using centre manifold reduction it is demonstrated that both models, although mathematically different, obey the same transcritical bifurcation pattern in the neighbourhood of the bifurcation point corresponding to the critical value of shock speed, the speed of sound.

Mathematics Subject Classification: 35L65, 35L67, 37G10, 34C37, 58K25

1. Introduction

Shock waves are moving singular surfaces on which jump discontinuities of field variables occur. In physical reality, due to dissipative mechanisms they are observed as narrow transition regions with steep gradients of field variables within, i.e. shock waves are endowed with structure. The shock structure problem consists of a mathematical description of this region

through particular solutions of appropriate mathematical models. This problem is challenging both from the mathematical and physical points of view. Mathematically, questions of existence and uniqueness are very important for the solutions with jump discontinuities, as well as for continuous ones. Physically, the continuum hypothesis becomes doubtful in this situation, thus limiting the range of validity of continuum theories of fluids.

This paper presents a contribution towards understanding common properties that may be found in descriptions of the shock structure within different continuum models of gas dynamics. It is motivated by the coexistence of the models with strikingly different mathematical structure, but pretending to describe the same phenomenon. In particular, the main issue of the study will be stability and bifurcation analysis of equilibrium states which naturally arises within the framework of the shock structure problem. The models to be discussed will be: (a) Euler's equations of gas dynamics, as a prototype of the hyperbolic system of conservation laws; (b) the Navier–Stokes–Fourier (NSF) parabolic model; (c) 13 moments equations, as a hyperbolic model with balance laws which arise within the context of extended thermodynamics.

Classical Euler's equations predict the existence of shock waves as discontinuous solutions travelling at a constant shock speed s. The jumps of field variables are related to the shock speed through the Rankine–Hugoniot equations [8]. Since their solution is not unique, an additional criterion has to be established in order to pick up physically admissible solutions. In this case Lax's condition, as well as other ones, claims that admissible weak shocks are the ones whose speed is supersonic with respect to the upstream equilibrium state [10, 26].

In contrast to Euler's model where dissipation is neglected, NSF equations take dissipative mechanisms into account through the classical constitutive equations for stress tensor and heat flux. Although the resulting mathematical model is parabolic, it has solutions in the form of a travelling wave which resemble the shock wave. They represent the shock with a structure which travels at a constant speed s, related to upstream and downstream equilibria through the same Rankine–Hugoniot equations as in Euler's model. The existence of such solutions is discussed for general parabolic models [21], and for this particular one as well [12, 19]. Using a travelling wave ansatz a system of partial differential equations (PDEs) is transformed into a system of ordinary differential equations (ODEs). In terms of phase trajectories of dynamical systems, the shock structure is then described as a heteroclinic orbit which asymptotically connects stationary points which correspond to equilibrium states of the model [13].

Another description of dissipative mechanisms in gas dynamics had been developed in the framework of extended thermodynamics [22]. It led to the so-called 13 moments model. The behaviour of nonconvective fluxes, like stress tensor and heat flux, is determined by additional balance laws. The differential part of the resulting system of balance laws is hyperbolic, at least in some region of the state space, but Rankine–Hugoniot equations have a different structure than in Euler's case. However, travelling waves—i.e. the shocks with a structure—may be constructed and their existence is related again to the shock waves which appear in Euler's model. This is in accordance with the existence result for hyperbolic systems of balance laws [31]. As in the NSF model, travelling shock profiles can be interpreted in terms of heteroclinic orbits connecting the same stationary points, although the ODE system governing the trajectories is different from the NSF one.

The existence theorems, either in the parabolic, or in the hyperbolic case, relate the existence of the shock profile to the following conditions:

(i) the upstream and downstream equilibrium states are related to the shock speed s through Rankine–Hugoniot equations for the basic (Euler's) model with neglected dissipation;

(ii) the pair of states connected by the shock profile satisfy the appropriate shock admissibility criterion, e.g. Lax's or Liu's condition, for the basic hyperbolic system without dissipation.

In particular, admissibility condition (ii), in its various forms, stands as a necessary and/or sufficient condition for the existence of shock profiles of weak shocks in general systems of conservation laws with viscous extensions (see [21], theorem 3.1), as well as in hyperbolic systems with relaxation (see [31], theorem 2.2).

The aim of this study is to analyse the shock structure problem using the dynamical systems approach [24]. The main idea is to drop the second condition (admissibility criterion) and to analyse the behaviour of the stationary points, i.e. upstream and downstream equilibrium states, while the shock speed is changed as a parameter. Using stability theory it will be shown that the stationary points change their stability properties while shock speed crosses the critical value which corresponds to the upstream speed of sound, determined from Euler's model. To be precise, one of the eigenvalues of the linearized system of ODEs describing the shock structure changes the sign in this situation. Furthermore, using centre manifold reduction and local bifurcation theory it will be shown that the stationary points form two transverse branches of solutions while the shock speed is varied. The one which corresponds to the downstream equilibrium state may be treated as a bifurcating solution. The local structure of solutions is then determined by the transcritical bifurcation pattern whose normal form is

$$\dot{y} = \epsilon y - y^2, \tag{1.1}$$

where y stands for a generic state variable and ϵ is a generic bifurcation parameter. These results will turn out to be valid both for the parabolic NSF model and for the hyperbolic 13 moments equations, i.e. the bifurcation equation will have the same form in either case. Thus, by putting the admissibility criterion aside it will be demonstrated that the existence of heteroclinic orbits is not a prerogative of admissible equilibrium states—they can also be observed in the case of inadmissible ones which appear in the case of subsonic wave speed. However, the stability criterion provided in this survey selects the admissible shock structures in dissipative models in an analogous way as the usual admissibility criteria do for shocks in Euler's system.

Stability and bifurcation analysis related to the shock structure problem had been applied mostly in the context of the Boltzmann equation. Nicolaenko and Thurber [23] showed that the Boltzmann operator for hard sphere potential has a nontrivial eigenvalue which changes the sign in transition from the subsonic to the supersonic regimes. Moreover, they derived bifurcation equations using the Lyapunov–Schmidt reduction procedure. Caflisch and Nicolaenko [7] generalized these results for hard cut-off potentials and proved the existence of shock profile solutions. Existence results for discrete velocity models of the Boltzmann equation, which also have a flavour of bifurcation theory, have been proven by Bose *et al* [4] and Bernhoff and Bobylev [5]. Recently [19], centre manifold reduction has been applied to prove the existence of weak shocks for the NSF model, and bifurcation equation of the transcritical type appeared there only as a by-product. On the other hand, bifurcation theory has been successfully applied to the analysis of the Riemann problem for viscous conservation laws [25] and bifurcation of undercompressive and overcompressive viscous profiles from the constant state [2]. However, it seems that there is a lack of comparative analysis of dissipative models which, although mathematically different, should have a common ground. This study tends to fill this gap and presents a continuation of the author's previous work [27].

The paper will be organized as follows. In section 2 the necessary background material about continuum models of gas dynamics and their mathematical structure will be presented. Section 3 will contain a brief survey of the centre manifold reduction procedure needed for local stability and bifurcation analysis. Section 4 will comprise a preparatory review of the shock wave analysis for Euler's equations. Key results on the shock structure analysis for the NSF model and the 13 moments equations in the light of dynamical systems theory will be presented

in sections 5 and 6. Finally, section 7 will contain a material which explains possible further applications of the method concerned with more involved mathematical models, as well as some numerical aspects of presented results.

2. Continuum models of gas dynamics

Continuum models in physics are often expressed in the form of conservation laws. When restricted to one space dimension they read

$$\partial_t \boldsymbol{F}^0(\boldsymbol{u}) + \partial_x \boldsymbol{F}(\boldsymbol{u}) = \boldsymbol{0}, \tag{2.1}$$

where $\boldsymbol{u} \in \boldsymbol{R}^n$, $\boldsymbol{u} = \boldsymbol{u}(x,t)$, is the vector of state variables; $\boldsymbol{F}^0(\boldsymbol{u})$ is the vector of densities and $\boldsymbol{F}(\boldsymbol{u})$ the vector of fluxes, both being smooth vector-functions in an open set of the state space. Physically, $\boldsymbol{F}(\boldsymbol{u})$ expresses the flux of the state variables through the boundary of some region in space and determines the rate of change of densities $\boldsymbol{F}^0(\boldsymbol{u})$, i.e. the state variables in it. The structure of the flux vector depends on the model of continuum adopted in a particular problem. A classical example is the Euler's system of gas dynamics equations

$$\begin{aligned} &\partial_t \rho + \partial_x(\rho v) = 0, \\ &\partial_t(\rho v) + \partial_x(\rho v^2 - \sigma + p) = 0, \\ &\partial_t(\tfrac{1}{2}\rho v^2 + \rho e) + \partial_x((\tfrac{1}{2}\rho v^2 + \rho e)v - \sigma v + pv + q) = 0. \end{aligned} \tag{2.2}$$

Viscous stress σ and heat flux q are neglected in this model ($\sigma = 0$, $q = 0$) and appear in equation (2.2) just for future reference. In what follows, the following set of state variables will be used $\boldsymbol{u} = (\rho, v, T)$, i.e. density, velocity and temperature. At the same time pressure p and internal energy density e are determined by the constitutive equations—thermal and caloric equations of state of an ideal gas

$$p = p(\rho, T) = R\rho T, \qquad e = e(\rho, T) = R\frac{T}{\gamma - 1}, \tag{2.3}$$

where $R = k_B/m$ is the gas constant (k_B is Boltzmann constant, m is the atomic mass of gas) and γ the ratio of specific heats.

When densities $\boldsymbol{F}^0(\boldsymbol{u})$ and fluxes $\boldsymbol{F}(\boldsymbol{u})$ are functions of state variables solely, i.e. not of their derivatives, it is expected that (2.1) is hyperbolic, at least in some region of the state space. In other words, the eigenvalue problem

$$\begin{aligned} &(-\lambda \boldsymbol{A}^0(\boldsymbol{u}) + \boldsymbol{A}(\boldsymbol{u}))\boldsymbol{r} = \boldsymbol{0}; \\ &\boldsymbol{A}^0(\boldsymbol{u}) = \partial \boldsymbol{F}^0(\boldsymbol{u})/\partial \boldsymbol{u}; \qquad \boldsymbol{A}(\boldsymbol{u}) = \partial \boldsymbol{F}(\boldsymbol{u})/\partial \boldsymbol{u}, \end{aligned} \tag{2.4}$$

has n real eigenvalues $\lambda_i(\boldsymbol{u})$ called characteristic speeds, and n linearly independent eigenvectors $\boldsymbol{r}_i(\boldsymbol{u})$, $i = 1, \ldots, n$; $\boldsymbol{A}^0(\boldsymbol{u})$ is assumed to be nonsingular. This property permits propagation of disturbances (waves) through space with finite speeds. In the usual terminology of hyperbolic conservation laws, $\lambda_i(\boldsymbol{u})$ is genuinely nonlinear if $(\partial\lambda_i(\boldsymbol{u})/\partial \boldsymbol{u}) \cdot \boldsymbol{r}_i(\boldsymbol{u}) \neq 0$ for all $\boldsymbol{u}$, while it is linearly degenerate if $(\partial\lambda_i(\boldsymbol{u})/\partial \boldsymbol{u}) \cdot \boldsymbol{r}_i(\boldsymbol{u}) = 0$ for all $\boldsymbol{u}$.

Hyperbolicity is the main cause of nonexistence of smooth solutions for all t, even when initial data are smooth. Jump discontinuities, i.e. shock waves, which are located on the surface of discontinuity $\Sigma(x,t)$, may appear in a finite time interval. If $[\![\cdot]\!] = (\cdot)_1 - (\cdot)_0$ denotes the jump of any quantity in front $(\cdot)_0$ and behind $(\cdot)_1$ the surface Σ, then Rankine–Hugoniot conditions relate the jump of the field variables to the speed of shock s

$$[\![\boldsymbol{F}(\boldsymbol{u})]\!] = s[\![\boldsymbol{F}^0(\boldsymbol{u})]\!]. \tag{2.5}$$

However, not all of the jump discontinuities which satisfy (2.5) are observable in reality (at least in the approximate sense). Along with Rankine–Hugoniot conditions, they have to

satisfy additional ones which serve as selection rules for physically admissible solutions. A review of these conditions may be found in [10, 26]. For the purpose of this exposition we shall be confined with the Lax condition

$$\lambda_i(\boldsymbol{u}_1) \geqslant s \geqslant \lambda_i(\boldsymbol{u}_0). \tag{2.6}$$

The study will be restricted to classical compressive i-shocks for which strict inequalities in (2.6) hold. In such a case the Lax condition represents a particular form of irreversibility condition since the roles of $\boldsymbol{u}_0$ and $\boldsymbol{u}_1$ cannot be interchanged [10]. A similar restriction comes from the entropy shock admissibility condition which puts this problem on a sound physical ground, but it is equivalent to (2.6) for weak i-shocks under certain assumptions.

Euler's equations (2.2) are equipped with the following set of characteristic speeds

$$\lambda_1 = v - c_s; \qquad \lambda_2 = v; \qquad \lambda_3 = v + c_s; \tag{2.7}$$

$$c_s = (\gamma RT)^{1/2}, \tag{2.8}$$

where c_s is the local speed of sound; λ_1 and λ_3 are genuinely nonlinear, whereas λ_2 is linearly degenerate. Lax condition (2.6) states that shock waves have to be supersonic w.r.t. the upstream state $\boldsymbol{u}_0 = (\rho_0, v_0, T_0)$ in front of them, and subsonic w.r.t. the downstream state $\boldsymbol{u}_1 = (\rho_1, v_1, T_1)$ behind them.

A flavour of bifurcation theory in the analysis of shock waves had been captured in the paper of Lax [18]. It may be outlined through the following observation. First, it is obvious that (2.5) has trivial solution $\boldsymbol{u}_1 = \boldsymbol{u}_0$ for any value of shock speed. Second, it may be shown by means of the implicit function theorem (see [22], p.189) that uniqueness of the trivial solution is lost when $s = \lambda_i(\boldsymbol{u}_0)$. Actually, Lax has shown that solution $\boldsymbol{u}_1 \neq \boldsymbol{u}_0$ of equation (2.5) belongs to the set of points known as the Hugoniot locus of $\boldsymbol{u}_0$ [10], thus representing the i-shock. Therefore, $\boldsymbol{u}_1$ may be regarded as a bifurcating solution when shock speed crosses the critical value $s^* = \lambda_i(\boldsymbol{u}_0) = \lambda_i(\boldsymbol{u}_1)$.

Existence of shock waves is an intrinsic property of hyperbolic systems of conservation laws such as (2.1). In reality they are recognized as narrow transition regions in the neighbourhood of surface of discontinuity $\Sigma(x, t)$ where steep gradients of the state variables occur, rather than their jumps. In such a way shock is endowed with the structure due to the presence of dissipative mechanisms, and a shock profile is observed instead of a shock wave.

Regularizing effects of dissipation can be modelled in several ways. Classical continuum mechanics motivates the so-called viscosity approach which regularizes system (2.1) by adding parabolic terms

$$\partial_t \boldsymbol{F}^0(\boldsymbol{u}) + \partial_x \boldsymbol{F}(\boldsymbol{u}) = \varepsilon \partial_x (\boldsymbol{B}(\boldsymbol{u}) \partial_x \boldsymbol{u}), \tag{2.9}$$

where $\boldsymbol{B}(\boldsymbol{u})$ is the viscosity matrix and $\varepsilon \in \boldsymbol{R}^+$ a small parameter. This model predicts infinite speed of propagation of disturbances, and characteristic speeds, as one of the basic features of a hyperbolic model (2.1), cannot be related to (2.9). However, parabolic terms regularize the shock waves which correspond to genuinely nonlinear characteristic speeds of (2.1). In such a way (2.9) comprises solutions representing the shock profile travelling uniformly with the shock speed s. For example, Euler's equations (2.2) are regularized when viscosity and heat conduction are taken into account through Navier–Stokes and Fourier constitutive equations

$$\sigma = \tfrac{4}{3}\mu \partial_x v, \qquad q = -\kappa \partial_x T, \tag{2.10}$$

where μ is viscosity of a gas and κ its heat conductivity ($\mu, \kappa > 0$). Consequently, the NSF model of gas dynamics reads

$$\begin{aligned}
&\partial_t \rho + \partial_x(\rho v) = 0,\\
&\partial_t(\rho v) + \partial_x(\rho v^2 + p) = \partial_x(\tfrac{4}{3}\mu\partial_x v),\\
&\partial_t(\tfrac{1}{2}\rho v^2 + \rho e) + \partial_x((\tfrac{1}{2}\rho v^2 + \rho e)v + pv)\\
&\quad = \partial_x(\kappa\partial_x T + \tfrac{4}{3}\mu v\partial_x v).
\end{aligned} \tag{2.11}$$

General considerations about the viscosity approach to weak shocks in systems of conservation laws are presented by Majda and Pego [21]. Existence and uniqueness of shock profile solutions for the NSF model (2.11) had been studied successfully by Gilbarg [12] for a rather general class of fluids where μ and κ are arbitrary functions of state variables.

Another way of describing dissipative mechanisms is to take into account the relaxation effects. Formally, this calls for extension of the set of state variables $\boldsymbol{u} \in \boldsymbol{R}^n$ by $\boldsymbol{v} \in \boldsymbol{R}^k$, $n + k = N$, which are governed by the additional set of balance laws. In particular, we have

$$\partial_t \hat{\boldsymbol{F}}^0(\boldsymbol{U}) + \partial_x \hat{\boldsymbol{F}}(\boldsymbol{U}) = \frac{1}{\tau}\boldsymbol{Q}(\boldsymbol{U}), \tag{2.12}$$

where

$$\begin{aligned}
&\boldsymbol{U} = \begin{pmatrix}\boldsymbol{u}\\ \boldsymbol{v}\end{pmatrix}, \qquad \boldsymbol{Q}(\boldsymbol{U}) = \begin{pmatrix}\boldsymbol{0}\\ \boldsymbol{q}(\boldsymbol{u},\boldsymbol{v})\end{pmatrix},\\
&\hat{\boldsymbol{F}}^0(\boldsymbol{U}) = \begin{pmatrix}\boldsymbol{f}^0(\boldsymbol{u},\boldsymbol{v})\\ \boldsymbol{g}^0(\boldsymbol{u},\boldsymbol{v})\end{pmatrix}, \qquad \hat{\boldsymbol{F}}(\boldsymbol{U}) = \begin{pmatrix}\boldsymbol{f}(\boldsymbol{u},\boldsymbol{v})\\ \boldsymbol{g}(\boldsymbol{u},\boldsymbol{v})\end{pmatrix},
\end{aligned} \tag{2.13}$$

and $\tau \in \boldsymbol{R}^+$ is a small parameter. It is assumed that $\boldsymbol{q}(\boldsymbol{u},\boldsymbol{v}) = \boldsymbol{0}$ uniquely determines 'the equilibrium manifold' $\boldsymbol{v}_{\mathrm{E}} = \boldsymbol{h}(\boldsymbol{u})$ as $\tau \to 0$, on which system (2.12) reduces to (2.1) with $\boldsymbol{F}^0(\boldsymbol{u}) = \boldsymbol{f}^0(\boldsymbol{u}, \boldsymbol{h}(\boldsymbol{u}))$ and $\boldsymbol{F}(\boldsymbol{u}) = \boldsymbol{f}(\boldsymbol{u}, \boldsymbol{h}(\boldsymbol{u}))$. In (2.12) the first n equations are conservation laws, while the remaining k ones are balance laws with source terms $\boldsymbol{q}(\boldsymbol{u},\boldsymbol{v})/\tau$ which describe the dissipative effects out of the equilibrium manifold.

It is customary to expect that system (2.12) is hyperbolic at least in some subset of the extended state space $\boldsymbol{R}^N$ which contains the equilibrium manifold. Corresponding characteristic speeds $\Lambda_j(\boldsymbol{U})$, $j = 1, \ldots, N$, and the set of linearly independent eigenvectors $\boldsymbol{R}_j(\boldsymbol{U})$ are determined from the eigenvalue problem for the differential part of (2.12)

$$\begin{aligned}
&(-\Lambda\hat{\boldsymbol{A}}^0(\boldsymbol{U}) + \hat{\boldsymbol{A}}(\boldsymbol{U}))\boldsymbol{R} = \boldsymbol{0};\\
&\hat{\boldsymbol{A}}^0(\boldsymbol{U}) = \partial\hat{\boldsymbol{F}}^0(\boldsymbol{U})/\partial\boldsymbol{U}; \qquad \hat{\boldsymbol{A}}(\boldsymbol{U}) = \partial\hat{\boldsymbol{F}}(\boldsymbol{U})/\partial\boldsymbol{U}.
\end{aligned} \tag{2.14}$$

An important property of characteristic speeds $\Lambda_j(\boldsymbol{U})$ is that they provide bounds for the characteristic speeds of (2.1) on equilibrium manifold through the subcharacteristic condition

$$\min_{1\leqslant j\leqslant N} \Lambda_j(\boldsymbol{u}, \boldsymbol{h}(\boldsymbol{u})) \leqslant \lambda_i(\boldsymbol{u}) \leqslant \max_{1\leqslant j\leqslant N} \Lambda_j(\boldsymbol{u}, \boldsymbol{h}(\boldsymbol{u})). \tag{2.15}$$

However, the spectrum $\lambda_i(\boldsymbol{u})$ of system (2.1) does not have to be contained in the spectrum $\Lambda_j(\boldsymbol{u}, \boldsymbol{h}(\boldsymbol{u}))$ of the hyperbolic dissipative system (2.12), i.e. λ's may not coincide with Λ's on the equilibrium manifold. Moreover, Rankine–Hugoniot conditions for (2.12) have a different form than for (2.1), and consequently may predict jump discontinuities which appear off the equilibrium manifold. These discrepancies between hyperbolic systems and their dissipative counterparts call for the answer to the question of how one can relate the jump discontinuities of (2.1) to the shock structure solutions expected to be derived from (2.12). First results may

be found in the work of Liu [20] for systems of two balance laws. The general existence result has been given by Yong and Zumbrun [31], under certain reasonable structural conditions.

In physical examples nonequilibrium variables v usually represent nonconvective fluxes such as stress tensor or heat flux, or even higher order moments in the framework of the kinetic theory of gases. The main example which we shall examine is the hyperbolic model of viscous, heat-conducting monatomic gas ($\gamma = 5/3$) obtained within the context of extended thermodynamics [22] and known as the 13 moments model. This model is the same as the 13 moments model of Grad [14] obtained in the kinetic theory of gases using a different closure procedure. Governing equations of this model have the form

$$\begin{aligned}
&\partial_t \rho + \partial_x(\rho v) = 0,\\
&\partial_t(\rho v) + \partial_x(\rho v^2 - \sigma + p) = 0,\\
&\partial_t\left(\frac{1}{2}\rho v^2 + \rho e\right) + \partial_x\left(\left(\frac{1}{2}\rho v^2 + \rho e\right)v - \sigma v + pv + q\right) = 0,\\
&\partial_t\left(\rho v^2 + p - \sigma\right) + \partial_x\left(\rho v^3 + 3pv - 3\sigma v + \frac{6}{5}q\right) = \frac{1}{\tau_\sigma}\sigma,\\
&\partial_t\left(\frac{1}{2}\rho v^3 + \frac{5}{2}pv - \sigma v + q\right)\\
&\quad +\partial_x\left(\frac{1}{2}\rho v^4 + 4pv^2 - \frac{5}{2}\sigma v^2 + \frac{16}{5}qv - \frac{7}{2}\frac{p}{\rho}\sigma + \frac{5}{2}\frac{p^2}{\rho}\right)\\
&\quad = -\frac{1}{\tau_q}\left(q - \frac{3}{2}\sigma v\right).
\end{aligned} \tag{2.16}$$

In this model stress σ and heat flux q are governed by the last two balance laws rather than constitutive equations (2.10). Small parameters τ_σ and τ_q play the role of relaxation times and, for monatomic gases, obey the relation $\tau_q = 3\tau_\sigma/2$. Although the models (2.11) and (2.16) are principally different, they are related to each other through the Chapman–Enskog expansion. Moreover, constitutive equations (2.10) can be recovered from balance laws of (2.16) by means of the Maxwellian iteration procedure (see [22]). Either of these methods leads to the following relations

$$\tau_\sigma = \frac{\mu}{p}, \qquad \tau_q = \frac{2}{5}\frac{\kappa}{p^2}\rho T, \qquad \kappa = \frac{15}{4}R\mu, \tag{2.17}$$

valid for monatomic gases.

Equilibrium manifold for the 13 moments system (2.16) is determined by $v_E = (\sigma_E, q_E) = (0, 0)$. Therefore, on v_E this system is reduced to the so-called equilibrium subsystem of the Euler's equations (2.2). The model (2.16) has five distinct characteristic speeds. When calculated in equilibrium and expressed in terms of sound speed (2.8) for monatomic gases ($\gamma = 5/3$) they read

$$\begin{aligned}
&\Lambda_1 = v - 1.6503c_s; \qquad \Lambda_2 = v - 0.6297c_s;\\
&\Lambda_3 = v;\\
&\Lambda_4 = v + 0.6297c_s; \qquad \Lambda_5 = v + 1.6503c_s.
\end{aligned} \tag{2.18}$$

All of them are genuinely nonlinear except Λ_3 which is linearly degenerate. Obviously, characteristic speeds (2.7) and (2.18) satisfy the subcharacteristic condition (2.15) on the equilibrium manifold with strict inequalities.

In stability and bifurcation analysis in sections 4–6 we shall be concerned with the models (2.2), (2.11) and (2.16).

3. Centre manifold reduction

To recognize the type of bifurcation which appears in a particular problem one does not have to analyse the behaviour of the whole set of state variables. Instead, the dimension of the state space can be reduced so that the reduced system comprises all the features of the original one in the neighbourhood of the critical point. The centre manifold theorem provides a systematic procedure for reducing the dimension of the state space. The theorem and some of its consequences useful for further analysis will be presented in this section. Although some of the symbols used here coincide with the ones from the previous section, there is no relation between them whatsoever.

Consider a dynamical system

$$\dot{\boldsymbol{x}} = \boldsymbol{X}(\boldsymbol{x}), \qquad \boldsymbol{x} \in \boldsymbol{R}^n, \tag{3.1}$$

and assume $\boldsymbol{x} = \boldsymbol{0}$ is its stationary point, $\boldsymbol{X}(\boldsymbol{0}) = \boldsymbol{0}$. Let $\boldsymbol{A} = D\boldsymbol{X}(\boldsymbol{0})$ be the Jacobian matrix. Its spectrum could be divided into three parts—stable σ_s, centre σ_c and unstable σ_u—depending on the sign of the real part of the eigenvalue λ

$$\begin{aligned} &\lambda \in \sigma_s \qquad \text{if } \operatorname{Re}\lambda < 0; \\ &\lambda \in \sigma_c \qquad \text{if } \operatorname{Re}\lambda = 0; \\ &\lambda \in \sigma_u \qquad \text{if } \operatorname{Re}\lambda > 0. \end{aligned} \tag{3.2}$$

Denote by E^s, E^c and E^u eigenspaces of σ_s, σ_c and σ_u, respectively. Then the following centre manifold theorem holds [16].

Theorem 3.1. *Let $\boldsymbol{X}(\boldsymbol{x})$ be a C^r vector function on $\boldsymbol{R}^n$, $\boldsymbol{X}(\boldsymbol{0}) = \boldsymbol{0}$. Then there exist C^r stable and unstable invariant manifolds W^s and W^u tangent to E^s and E^u at $\boldsymbol{0}$ and a C^{r-1} centre manifold W^c tangent to E^c at $\boldsymbol{0}$. The manifolds W^s, W^u and W^c are all invariant for trajectories of system (3.1).*

In order to enable effective calculation of the centre manifold, needed to determine the bifurcation pattern, a local coordinate chart has to be chosen. Assume that $\boldsymbol{x} = (\boldsymbol{y}, \boldsymbol{z})$, $\boldsymbol{y} \in \boldsymbol{R}^k$, $\boldsymbol{z} \in \boldsymbol{R}^m$, $k + m = n$, puts the linear part of (3.1) at $\boldsymbol{0}$ into block diagonal form

$$\begin{aligned} \dot{\boldsymbol{y}} &= \boldsymbol{B}\boldsymbol{y} + \boldsymbol{Y}(\boldsymbol{y}, \boldsymbol{z}); \\ \dot{\boldsymbol{z}} &= \boldsymbol{C}\boldsymbol{z} + \boldsymbol{Z}(\boldsymbol{y}, \boldsymbol{z}), \end{aligned} \tag{3.3}$$

where $\boldsymbol{B}$ and $\boldsymbol{C}$ are constant square matrices whose eigenvalues have zero and nonzero real parts, respectively, and $\boldsymbol{Y}$ and $\boldsymbol{Z}$ vanish along with their first derivatives at $\boldsymbol{0}$. Since the centre manifold is tangent to E^c it can be represented as

$$W^c = \{(\boldsymbol{y}, \boldsymbol{z}) : \boldsymbol{z} = \boldsymbol{h}(\boldsymbol{y})\}; \qquad \boldsymbol{h}(\boldsymbol{0}) = \boldsymbol{0},\ D\boldsymbol{h}(\boldsymbol{0}) = \boldsymbol{0}, \tag{3.4}$$

where $\boldsymbol{h}(\boldsymbol{y})$ is defined in some neighbourhood of $\boldsymbol{0} \in \boldsymbol{R}^k$. Therefore, dynamics of system (3.3) can be reduced to W^c in the neighbourhood of the origin by means of the following equation:

$$\dot{\boldsymbol{y}} = \boldsymbol{B}\boldsymbol{y} + \boldsymbol{Y}(\boldsymbol{y}, \boldsymbol{h}(\boldsymbol{y})). \tag{3.5}$$

The actual form of $\boldsymbol{h}(\boldsymbol{y})$ is determined from the equation for $\boldsymbol{z}$ in (3.3)

$$D\boldsymbol{h}(\boldsymbol{y})\left[\boldsymbol{B}\boldsymbol{y} + \boldsymbol{Y}(\boldsymbol{y}, \boldsymbol{h}(\boldsymbol{y}))\right] - \boldsymbol{C}\boldsymbol{h}(\boldsymbol{y}) + \boldsymbol{Z}(\boldsymbol{y}, \boldsymbol{h}(\boldsymbol{y})) = \boldsymbol{0}, \tag{3.6}$$

along with boundary conditions $\boldsymbol{h}(\boldsymbol{0}) = \boldsymbol{0}$, $D\boldsymbol{h}(\boldsymbol{0}) = \boldsymbol{0}$. The system of PDEs (3.6) can hardly be solved exactly. However, $\boldsymbol{h}(\boldsymbol{y})$ can usually be approximated to a desired degree of accuracy by Taylor series expansion at $\boldsymbol{y} = \boldsymbol{0}$.

The importance of centre manifold could be illustrated by a simple example (see [16]). For a two-dimensional system

$$\dot{y} = yz; \qquad \dot{z} = -z - y^2, \tag{3.7}$$

tangent space approximation $z = h(y) = 0$, motivated by the fact that $z \to 0$ as $t \to \infty$ in linear approximation, leads to $\dot{y} = 0$ which does not provide any information about stability near the origin 0. However, second order centre manifold approximation

$$z = h(y) = -y^2 + O(y^4) \tag{3.8}$$

determines the reduced system

$$\dot{y} = -y^3 + O(y^5) \tag{3.9}$$

which shows that 0 is a stable stationary point.

Centre manifold reduction can also be applied to systems which contain parameters. For simplicity assume that (3.1) depends upon a single parameter $\epsilon \in \boldsymbol{R}$. Application of the centre manifold theorem is devised through the simple extension of system (3.3)

$$\begin{aligned} \dot{\boldsymbol{y}} &= \boldsymbol{B}_\epsilon \boldsymbol{y} + \boldsymbol{Y}_\epsilon(\boldsymbol{y}, \boldsymbol{z}); \\ \dot{\boldsymbol{z}} &= \boldsymbol{C}_\epsilon \boldsymbol{z} + \boldsymbol{Z}_\epsilon(\boldsymbol{y}, \boldsymbol{z}); \\ \dot{\epsilon} &= 0. \end{aligned} \tag{3.10}$$

It has a $k+1$-dimensional centre manifold tangent to $(\boldsymbol{y}, \epsilon)$ space which may be approximated by $\boldsymbol{z} = \boldsymbol{h}(\boldsymbol{y}, \epsilon)$. This is standard procedure for calculating the bifurcation equation. For details about this suspension method and references to original papers see [16].

4. Shock waves in Euler's equations

The first step in the analysis will be the solution of Rankine–Hugoniot equations (2.5) for Euler's system (2.2). It is motivated by the fact that the shock structure is a continuous solution which connects equilibrium states. These equilibrium states are, on the other hand, related by Rankine–Hugoniot conditions for jump discontinuities.

Introducing relative velocity $u = v - s$, equation (2.5) for the Euler's system may be transformed into

$$\begin{aligned} &[\![\rho u]\!] = 0; \\ &[\![\rho u^2 + p]\!] = 0; \\ &[[(\tfrac{1}{2}\rho u^2 + \rho\varepsilon)u + pu]] = 0. \end{aligned} \tag{4.1}$$

Using constitutive equations (2.3), the following nontrivial solution is obtained [8]:

$$\begin{aligned} \frac{\rho_1}{\rho_0} &= \frac{M_0^2}{1 - \mu^2(1 - M_0^2)}; \\ \frac{u_1}{u_0} &= \frac{1}{M_0^2}[1 - \mu^2(1 - M_0^2)]; \\ \frac{T_1}{T_0} &= \frac{1}{M_0^2}[(1 - \mu^2(1 - M_0^2))((1 + \mu^2)M_0^2 - \mu^2)], \end{aligned} \tag{4.2}$$

where $M_0 = u_0/c_{s0}$ is the Mach number in the upstream equilibrium, c_{s0} being corresponding sound speed, and $\mu^2 = (\gamma - 1)/(\gamma + 1)$. It is important to note that the downstream state $\boldsymbol{u}_1$ tends to the upstream state $\boldsymbol{u}_0$ when $M_0 \to 1$, i.e. when the speed of shock tends to the highest characteristic speed (see figure 1). Therefore, the downstream equilibrium state $\boldsymbol{u}_1(\boldsymbol{u}_0, M_0)$

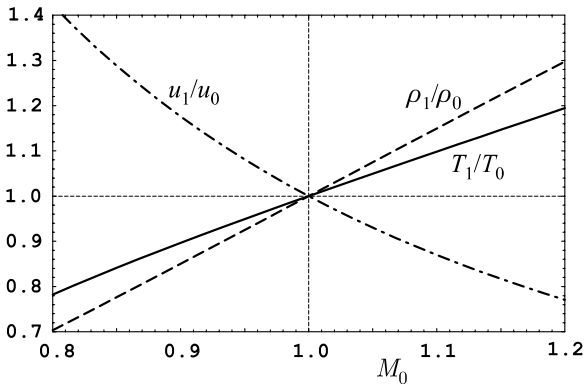

Figure 1. Solution of Rankine–Hugoniot equations for Euler's model ($\gamma = 5/3$).

can be regarded as a bifurcating solution, which is transverse to the trivial branch $\boldsymbol{u}_0$ in the neighbourhood of the critical point $M_0 = 1$. Note also that, according to Lax's condition (2.6), only the supersonic nontrivial branch ($M_0 > 1$) is physically admissible, whereas for $M_0 < 1$ the trivial branch ($\boldsymbol{u}_1 = \boldsymbol{u}_0$) is an admissible one.

5. Stability and bifurcation of equilibrium in NSF model

Since shock structure is regarded as a travelling wave which moves with the speed of shock s, the solution of the problem in the case of the parabolic dissipative model (2.9) will be assumed in the form $\boldsymbol{u}(x,t) = \hat{\boldsymbol{u}}(\xi)$, $\xi = (x - st)/\varepsilon$. In such a way the system of PDEs is reduced to the ODE system

$$(-s\boldsymbol{A}^0(\hat{\boldsymbol{u}}) + \boldsymbol{A}(\hat{\boldsymbol{u}}))\frac{\mathrm{d}\hat{\boldsymbol{u}}}{\mathrm{d}\xi} = \frac{\mathrm{d}}{\mathrm{d}\xi}\left(\boldsymbol{B}(\hat{\boldsymbol{u}})\frac{\mathrm{d}\hat{\boldsymbol{u}}}{\mathrm{d}\xi}\right), \tag{5.1}$$

where the small parameter ε disappeared due to scaling of the independent variable. It can be further simplified when the profile is considered in the frame of reference moving with a shock. Due to Galilean invariance of governing equations, the problem becomes stationary by introducing the relative velocity $u = v - s$ and equation (5.1) is reduced to

$$\boldsymbol{A}(\hat{\boldsymbol{u}})\frac{\mathrm{d}\hat{\boldsymbol{u}}}{\mathrm{d}\xi} = \frac{\mathrm{d}\boldsymbol{F}(\hat{\boldsymbol{u}})}{\mathrm{d}\xi} = \frac{\mathrm{d}}{\mathrm{d}\xi}\left(\boldsymbol{B}(\hat{\boldsymbol{u}})\frac{\mathrm{d}\hat{\boldsymbol{u}}}{\mathrm{d}\xi}\right), \tag{5.2}$$

which can be integrated to obtain

$$\boldsymbol{B}(\hat{\boldsymbol{u}})\frac{\mathrm{d}\hat{\boldsymbol{u}}}{\mathrm{d}\xi} = \boldsymbol{F}(\hat{\boldsymbol{u}}) - \boldsymbol{F}(\hat{\boldsymbol{u}}_0). \tag{5.3}$$

This set of ODEs is accompanied by boundary conditions

$$\begin{aligned} &\hat{\boldsymbol{u}}(-\infty) = \boldsymbol{u}_0; \qquad \hat{\boldsymbol{u}}(\infty) = \boldsymbol{u}_1; \\ &\frac{\mathrm{d}\hat{\boldsymbol{u}}(\pm\infty)}{\mathrm{d}\xi} = \boldsymbol{0}, \end{aligned} \tag{5.4}$$

where $\boldsymbol{u}_0$ and $\boldsymbol{u}_1$ are related through Rankine–Hugoniot equations (2.5). Equilibrium states $\boldsymbol{u}_0$ and $\boldsymbol{u}_1$ thus represent the stationary points of system (5.3) and the shock structure is a heteroclinic orbit connecting them.

5.1. Shock structure equations

The study of the shock structure problem in the NSF model will commence with the assumption that viscosity is not constant, but the power-law function of the temperature

$$\mu = \mu_0 (T/T_0)^\alpha, \tag{5.5}$$

where the exponent α depends on the type of gas in consideration and μ_0 is viscosity in the referent state, here being the upstream equilibrium. For the purpose of comparison, analysis will be restricted to the case of monatomic gases ($\gamma = 5/3$). The problem will be considered in a moving reference frame with a single independent variable $\xi = x - st$. The model will be put into dimensionless form using nondimensional quantities

$$\tilde{\xi} = \frac{\xi}{l_0}; \qquad \tilde{\rho} = \frac{\rho}{\rho_0}; \qquad \tilde{u} = \frac{v - s}{c_0}; \qquad \tilde{T} = \frac{T}{T_0}; \tag{5.6}$$
$$M_0 = \frac{v_0 - s}{c_0}; \qquad c_0 = \left(\frac{5}{3} R T_0\right)^{1/2}; \qquad l_0 = \frac{\mu_0}{\rho_0 R T_0} c_0,$$

where c_0 is the speed of sound in the upstream equilibrium and M_0 the corresponding Mach number. Reference length l_0 is related to the mean free path of gas atoms $\tilde{\lambda}$ through

$$\tilde{\lambda} = \sqrt{\frac{3}{5}} \frac{16}{5\sqrt{2\pi}} l_0 \approx 0.989 l_0, \tag{5.7}$$

which is quite desirable for numerical purposes and could give an indication about relation between shock thickness and mean free path. For the sake of simplicity tildes will be dropped in the following text.

Dimensionless equations describing the shock structure have the following form

$$\begin{aligned}
&\frac{\mathrm{d}}{\mathrm{d}\xi}(\rho u) = 0; \\
&\frac{\mathrm{d}}{\mathrm{d}\xi}\left(\frac{5}{3}\rho u^2 + \rho T\right) = \frac{\mathrm{d}}{\mathrm{d}\xi}\left(\frac{4}{3} T^\alpha \frac{\mathrm{d}u}{\mathrm{d}\xi}\right); \\
&\frac{\mathrm{d}}{\mathrm{d}\xi}\left(\frac{5}{6}\rho u^3 + \frac{5}{2}\rho T u\right) = \frac{\mathrm{d}}{\mathrm{d}\xi}\left(\frac{4}{3} T^\alpha u \frac{\mathrm{d}u}{\mathrm{d}\xi} + \frac{9}{4} T^\alpha \frac{\mathrm{d}T}{\mathrm{d}\xi}\right).
\end{aligned} \tag{5.8}$$

This system could be integrated once to obtain

$$\begin{aligned}
&\rho u = M_0; \\
&\frac{5}{3}(\rho u^2 - M_0) + \rho T - 1 = \frac{4}{3} T^\alpha \frac{\mathrm{d}u}{\mathrm{d}\xi}; \\
&\frac{5}{6}(\rho u^3 - M_0^3) + \frac{5}{2}(\rho T u - M_0) = \frac{4}{3} T^\alpha u \frac{\mathrm{d}u}{\mathrm{d}\xi} + \frac{9}{4} T^\alpha \frac{\mathrm{d}T}{\mathrm{d}\xi},
\end{aligned} \tag{5.9}$$

where dimensionless upstream equilibrium values

$$\rho_0 = 1; \qquad u_0 = M_0; \qquad T_0 = 1, \tag{5.10}$$

have been used. Eliminating ρ by the use of mass conservation, the following system of two first-order ODEs is obtained

$$\begin{aligned}
\frac{\mathrm{d}u}{\mathrm{d}\xi} &= F_{\mathrm{P}}(u, T, M_0) = \frac{1}{4T^\alpha}\left(-3 - 5M_0^2 + 3M_0 \frac{T}{u} + 5M_0 u\right); \\
\frac{\mathrm{d}T}{\mathrm{d}\xi} &= G_{\mathrm{P}}(u, T, M_0) = -\frac{2}{27T^\alpha}(5M_0(3 + M_0^2) - 9M_0 T \\
&\quad -2(3 + 5M_0^2)u + 5M_0^2 u^2).
\end{aligned} \tag{5.11}$$

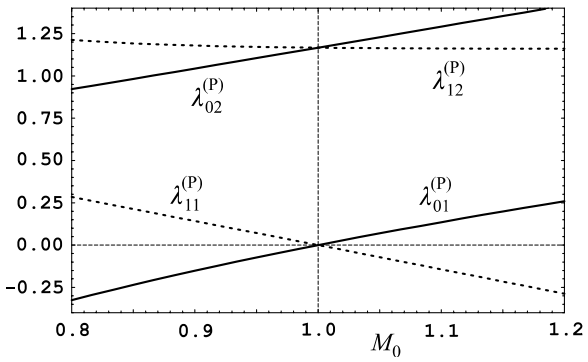

Figure 2. Graphs of the eigenvalues (A.2) and (A.5) in NSF model ($\alpha = 1$).

By straightforward calculation it can be checked that the downstream equilibrium state, calculated from (4.2)

$$u_1 = \frac{3 + M_0^2}{4M_0}; \qquad T_1 = \frac{1}{16}\left(14 - \frac{3}{M_0^2} + 5M_0^2\right), \tag{5.12}$$

determines another stationary point of (5.11), $F_{\mathrm{P}}(u_1, T_1, M_0) = 0$, $G_{\mathrm{P}}(u_1, T_1, M_0) = 0$.

5.2. Stability analysis of equilibrium points

The main idea of stability analysis is to show that stationary points (u_0, T_0) and (u_1, T_1) change their stability properties when parameter M_0 crosses its critical value $M_0 = 1$. For $M_0 \neq 1$ they are hyperbolic (in the sense of dynamical systems terminology), whereas hyperbolicity is lost for $M_0 = 1$, meaning that one of the eigenvalues determined from linearized equations changes its sign.

Theorem 5.1. *Let $\lambda_{0j}^{(P)}(M_0)$ and $\lambda_{1j}^{(P)}(M_0)$, $j = 1, 2$, denote the eigenvalues of the linearized system derived from (5.11) at the stationary points (u_0, T_0) and (u_1, T_1), respectively. There exists a neighbourhood of the critical value of the parameter $M_0 = 1$ such that one of the eigenvalues changes its sign. Precisely, the following inequalities hold*

$$\begin{aligned} &\lambda_{01}^{(P)}(M_0) < 0 < \lambda_{02}^{(P)}(M_0) && \text{for } M_0 < 1; \\ &0 < \lambda_{01}^{(P)}(M_0) < \lambda_{02}^{(P)}(M_0) && \text{for } M_0 > 1; \end{aligned} \tag{5.13}$$

$$\begin{aligned} &0 < \lambda_{11}^{(P)}(M_0) < \lambda_{12}^{(P)}(M_0) && \text{for } M_0 < 1; \\ &\lambda_{11}^{(P)}(M_0) < 0 < \lambda_{12}^{(P)}(M_0) && \text{for } M_0 > 1. \end{aligned} \tag{5.14}$$

The proof of the theorem is given in appendix A. Figure 2 shows graphs of the eigenvalues considered in stability analysis in the case $\alpha = 1$ and illustrates inequalities (5.13) and (5.14). It is easy to conclude that (u_0, T_0) is a saddle point in the subsonic case and an unstable node in the supersonic case, whereas (u_1, T_1) is an unstable node in the subsonic case and a saddle point in the supersonic case.

The character of stationary points in the NSF model in the supersonic case has been discussed by Gilbarg and Paolucci [13] and extensively used in construction of the shock profile. Figure 3 shows phase portraits of the dynamical system (5.11) in the subsonic ($M_0 = 0.8$) and supersonic ($M_0 = 1.2$) cases obtained by numerical simulation. They confirm the character of stationary points indicated by linear stability analysis. Heteroclinic orbits connecting them are indicated by the solid black line.

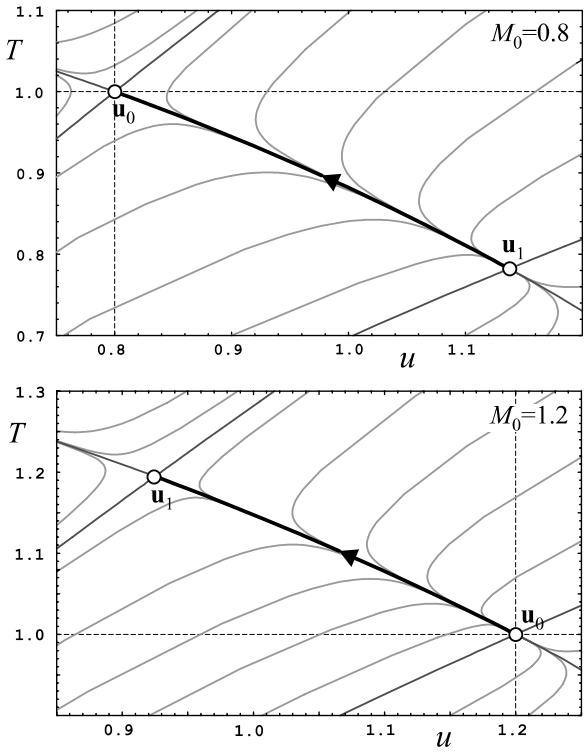

Figure 3. Phase portraits in NSF model in subsonic ($M_0 = 0.8$) and supersonic ($M_0 = 1.2$) case. Heteroclinic orbits indicated by a solid black line.

5.3. Local bifurcation analysis

The goal of local bifurcation analysis is to show that a transcritical bifurcation pattern can be observed in the neighbourhood of the critical value of the bifurcation parameter—Mach number $M_0 = 1$. The stationary point (u_0, T_0) will be treated as a basic solution and (u_1, T_1) as a bifurcating one. The analysis will be performed in several standard steps. First (lemma 5.1), system (5.11) will be transformed into a normal form in the neighbourhood of the stationary point (u_0, T_0). Second, the centre manifold will be determined in an approximate sense (lemma 5.2), as indicated in section 3. Finally, in theorem 5.2 the bifurcation equation will be derived revealing the bifurcation pattern.

Let Δu and ΔT denote perturbations of equilibrium values (5.10) of u and T and let $\Delta M_0 = M_0 - 1$. We have $u = 1 + \Delta M_0 + \Delta u$, $T = 1 + \Delta T$ and system (5.11) can be written in suspended form

$$\begin{aligned}
\frac{\mathrm{d}\Delta u}{\mathrm{d}\xi} &= F_{\mathrm{P}}(1 + \Delta M_0 + \Delta u, 1 + \Delta T);\\
\frac{\mathrm{d}\Delta T}{\mathrm{d}\xi} &= G_{\mathrm{P}}(1 + \Delta M_0 + \Delta u, 1 + \Delta T);\\
\frac{\mathrm{d}\Delta M_0}{\mathrm{d}\xi} &= 0.
\end{aligned} \tag{5.15}$$

Linearization of (5.15) at $(\Delta u, \Delta T, \Delta M_0) = (0, 0, \Delta M_0)$ reads

$$\hat{\boldsymbol{A}}_{\mathrm{P}0}(\Delta M_0) = \begin{pmatrix} \boldsymbol{A}_{\mathrm{P}0}(1 + \Delta M_0) & \boldsymbol{0} \\ \boldsymbol{0} & 0 \end{pmatrix}, \tag{5.16}$$

and

$$\hat{\boldsymbol{A}}_{\mathrm{P}0}(0) = \begin{pmatrix} 1/2 & 3/4 & 0 \\ 4/9 & 2/3 & 0 \\ 0 & 0 & 0 \end{pmatrix}. \tag{5.17}$$

Lemma 5.1. *By means of linear transformation*

$$(\Delta u, \Delta T, \Delta M_0) = (-\tfrac{3}{2}y + \tfrac{9}{8}z, y + z, \epsilon) \tag{5.18}$$

system (5.15) is transformed into normal form

$$\begin{aligned} \frac{\mathrm{d}}{\mathrm{d}\xi}\begin{pmatrix} y \\ z \\ \epsilon \end{pmatrix} &= \begin{pmatrix} f_{\mathrm{P}}(y, z, \epsilon) \\ g_{\mathrm{P}}(y, z, \epsilon) \\ 0 \end{pmatrix} \\ &= \boldsymbol{B}_{\mathrm{P}0}(\mu)\begin{pmatrix} y \\ z \\ \epsilon \end{pmatrix} + \begin{pmatrix} Y_{\mathrm{P}}(y, z, \epsilon) \\ Z_{\mathrm{P}}(y, z, \epsilon) \\ 0 \end{pmatrix}, \end{aligned} \tag{5.19}$$

where

$$\boldsymbol{B}_{\mathrm{P}0}(0) = \begin{pmatrix} 0 & 0 & 0 \\ 0 & 7/6 & 0 \\ 0 & 0 & 0 \end{pmatrix}, \tag{5.20}$$

and $Y_{\mathrm{P}}(y, z, \epsilon)$ and $Z_{\mathrm{P}}(y, z, \epsilon)$ vanish along with their first derivatives at $(0, 0, \epsilon)$.

The proof of the lemma is given in appendix A. The transformed system (5.19) has double zero eigenvalue at the origin and its centre subspace E^{c} is spanned by $\boldsymbol{e}_{\mathrm{P}1}$ and $\boldsymbol{e}_{\mathrm{P}3}$. As a consequence of (3.4) and (3.6), the centre manifold W^{c} has the general form

$$\begin{aligned} &z = h(y, \epsilon); \\ &h(0, 0) = 0; \qquad \frac{\partial h(0, 0)}{\partial y} = 0; \qquad \frac{\partial h(0, 0)}{\partial \epsilon} = 0, \end{aligned} \tag{5.21}$$

and has to satisfy the equation

$$\frac{\partial h(y, \epsilon)}{\partial y} f_{\mathrm{P}}(y, h(y, \epsilon), \epsilon) - g_{\mathrm{P}}(y, h(y, \epsilon), \epsilon) = 0. \tag{5.22}$$

Following the arguments of section 3, $h(y, \epsilon)$ will be approximated by Taylor series expansion in the neighbourhood of the origin. Using the second order approximation $h(y, \epsilon) \approx c_{yy}y^2 + c_{y\epsilon}y\epsilon + c_{\epsilon\epsilon}\epsilon^2$ one directly obtains the following result.

Lemma 5.2. *The centre manifold (5.21) which satisfies equation (5.22) can be approximated by*

$$h(y, \epsilon) \approx \frac{32}{49}\epsilon y - \frac{25}{49}y^2 \tag{5.23}$$

in the neighbourhood of the origin.

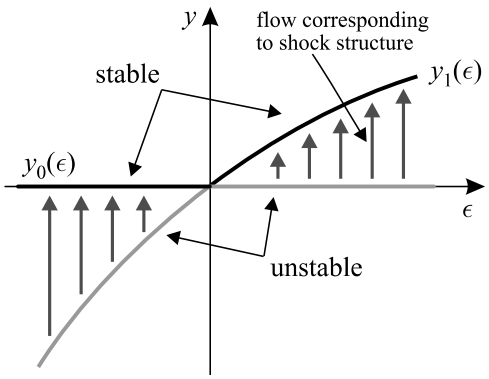

Figure 4. Bifurcation diagram of transcritical bifurcation pattern (5.24).

The bifurcation equation for this problem is obtained by inserting (5.23) into $\mathrm{d}y/\mathrm{d}\xi = f_{\mathrm{P}}(y, h(y,\epsilon),\epsilon)$. Expanding the result in Taylor series, the main result of the analysis is obtained.

Theorem 5.2. *Bifurcation of equilibrium* $(y, z, \epsilon) = (0, 0, \epsilon)$ *of (5.19) appears for the bifurcation value of parameter* $\epsilon = 0$ *and the corresponding bifurcation equation has the form*

$$\frac{\mathrm{d}y}{\mathrm{d}\xi} = \frac{10}{7}\epsilon y - \frac{20}{7}y^2 + O_3 \tag{5.24}$$

where O_3 *denotes terms which vanish along with their first and second derivatives with respect to* y *and* ϵ *for* $(y, \epsilon) = (0, 0)$.

In order to support this result, a qualitative structure of the bifurcation diagram corresponding to equation (5.24) is given in figure 4. One may observe that there exists the trivial solution branch $y_0(\epsilon) \equiv 0$ which corresponds to the upstream equilibrium state. It is stable for $\epsilon < 0$ and unstable for $\epsilon > 0$. On the other hand, the nontrivial solution branch $y_1(\epsilon) = \epsilon/2 + O(\epsilon^2)$ is transverse to y_0 and corresponds to downstream equilibrium. Stability properties of these solutions are indicated in the figure. The flow corresponding to the shock structure is transverse to both equilibrium branches and corresponds to heteroclinic orbits of the dynamical system (5.11).

Note that the stable branch of the bifurcating solution $y_1(\epsilon)$ corresponds to physically admissible solutions of Rankine–Hugoniot equations (4.1), in the sense of Lax. However, Lax's condition has not been exploited at all in stability and bifurcation analysis of this section. In such a way, stability considerations of theorem 5.1 seem to provide an equivalent condition as the Lax's one.

Although the local bifurcation analysis may blur a bit the original shock structure problem, it has some useful consequences. In section 7 it will be shown how an approximate solution can be constructed from the solution of bifurcation equation (5.24).

6. Stability and bifurcation of equilibrium in extended thermodynamics

In the case of the hyperbolic dissipative model (2.12) travelling shock profile is assumed in the form $\boldsymbol{U}(x,t) = \hat{\boldsymbol{U}}(\xi)$, $\xi = (x - st)/\tau$. The PDE system is thus reduced to the system of ODEs

$$(-s\hat{\boldsymbol{A}}^0(\hat{\boldsymbol{U}}) + \hat{\boldsymbol{A}}(\hat{\boldsymbol{U}}))\frac{\mathrm{d}\hat{\boldsymbol{U}}}{\mathrm{d}\xi} = \boldsymbol{Q}(\hat{\boldsymbol{U}}), \tag{6.1}$$

where the small parameter τ disappeared due to scaling of the independent variable. When the profile is considered in the moving frame of reference the problem becomes stationary due to Galilean invariance, and by introduction of the relative velocity $u = v - s$, equation (6.1) reduces it to

$$\hat{\boldsymbol{A}}(\hat{\boldsymbol{U}})\frac{\mathrm{d}\hat{\boldsymbol{U}}}{\mathrm{d}\xi} = \frac{\mathrm{d}\hat{\boldsymbol{F}}(\hat{\boldsymbol{U}})}{\mathrm{d}\xi} = \boldsymbol{Q}(\hat{\boldsymbol{U}}). \tag{6.2}$$

It is accompanied by the following boundary conditions:

$$\begin{aligned}
&\hat{\boldsymbol{U}}(-\infty) = \begin{pmatrix} \hat{\boldsymbol{u}}(-\infty) \\ \hat{v}(-\infty) \end{pmatrix} = \begin{pmatrix} \boldsymbol{u}_0 \\ \boldsymbol{h}(\boldsymbol{u}_0) \end{pmatrix}; \\
&\hat{\boldsymbol{U}}(\infty) = \begin{pmatrix} \hat{\boldsymbol{u}}(\infty) \\ \hat{v}(\infty) \end{pmatrix} = \begin{pmatrix} \boldsymbol{u}_1 \\ \boldsymbol{h}(\boldsymbol{u}_1) \end{pmatrix}; \\
&\frac{\mathrm{d}\hat{\boldsymbol{U}}(\pm\infty)}{\mathrm{d}\xi} = \boldsymbol{0}
\end{aligned} \tag{6.3}$$

where $\boldsymbol{u}_0$ and $\boldsymbol{u}_1$ are related by Rankine–Hugoniot conditions (2.5). Since these end states belong to the equilibrium manifold of (2.12), they are also the stationary points of system (6.2) and the shock structure is again the heteroclinic orbit connecting them.

6.1. Shock structure equations

To obtain dimensionless equations describing the shock structure in extended thermodynamics, the following non-dimensional quantities will be introduced in addition to (5.6)

$$\tilde{\sigma} = \frac{\sigma}{\rho_0 R T_0}; \qquad \tilde{q} = \frac{q}{\rho_0 R T_0 c_0}. \tag{6.4}$$

By dropping the tildes for convenience, one derives from (2.16) the following system of shock structure equations:

$$\begin{aligned}
&\frac{\mathrm{d}}{\mathrm{d}\xi}(\rho u) = 0; \\
&\frac{\mathrm{d}}{\mathrm{d}\xi}\left(\frac{5}{3}\rho u^2 + \rho T - \sigma\right) = 0; \\
&\frac{\mathrm{d}}{\mathrm{d}\xi}\left(\frac{5}{6}\rho u^3 + \frac{5}{2}\rho T u - \sigma u + q\right) = 0; \\
&\frac{\mathrm{d}}{\mathrm{d}\xi}\left(\frac{5}{3}\rho u^3 + 3\rho T u - 3\sigma u + \frac{6}{5}q\right) = \rho T^{1-\alpha}\sigma; \\
&\frac{\mathrm{d}}{\mathrm{d}\xi}\left(\frac{5}{6}\rho u^4 + 4\rho T u^2 - \frac{5}{2}\sigma u^2 + \frac{16}{5}q u - \frac{21}{10}T\sigma + \frac{3}{2}\rho T^2\right) \\
&\quad = -\frac{2}{3}\rho T^{1-\alpha}\left(q - \frac{3}{2}\sigma u\right).
\end{aligned} \tag{6.5}$$

In the derivation we used (2.17) and assumption (5.5). The first three equations could be integrated taking into account the equilibrium values at $x = -\infty$

$$\rho_0 = 1; \qquad u_0 = M_0; \qquad T_0 = 1; \qquad \sigma_0 = 0; \qquad q_0 = 0, \tag{6.6}$$

and used to express ρ, σ and q in terms of u, T and Mach number M_0 as parameter

$$\begin{aligned}
\rho &= \frac{M_0}{u};\\
\sigma &= \frac{5}{3}M_0(u-M_0)+M_0\frac{T}{u}-1;\\
q &= \frac{5}{6}M_0(M_0^2-u^2)+\frac{5}{2}M_0(1-T)+\frac{5}{3}M_0u(u-M_0)+M_0T-u.
\end{aligned} \tag{6.7}$$

In such a way system (6.5) is reduced to the system of two first-order ODEs

$$\frac{\mathrm{d}u}{\mathrm{d}\xi}=F_{\mathrm{H}}(u,T,M_0); \qquad \frac{\mathrm{d}T}{\mathrm{d}\xi}=G_{\mathrm{H}}(u,T,M_0), \tag{6.8}$$

where the right-hand sides have the following form

$$F_{\mathrm{H}}(u,T,M_0)=\frac{\Delta_u}{\Delta}; \qquad G_{\mathrm{H}}(u,T,M_0)=\frac{\Delta_T}{\Delta}, \tag{6.9}$$

for

$$\begin{aligned}
\Delta &= 1701T^{2\alpha}+12150M_0^2T^{2\alpha}+6885M_0^4T^{2\alpha}-2988M_0^2T^{1+2\alpha}\\
&\quad +486\frac{M_0^2T^{2+2\alpha}}{u^2}-972\frac{M_0T^{1+2\alpha}}{u}-1620\frac{M_0^3T^{1+2\alpha}}{u}\\
&\quad -11052M_0T^{2\alpha}u-18420M_0^3T^{2\alpha}u+12660M_0^2T^{2\alpha}u^2;\\
\Delta_u &= 4365M_0^2T^{1+\alpha}+7275M_0^4T^{1+\alpha}-540\frac{M_0^3T^{3+\alpha}}{u^3}\\
&\quad +1485\frac{M_0^2T^{2+\alpha}}{u^2}+2475\frac{M_0^4T^{2+\alpha}}{u^2}-945\frac{M_0T^{1+\alpha}}{u}\\
&\quad -4500\frac{M_0^3T^{1+\alpha}}{u}-3075\frac{M_0^5T^{1+\alpha}}{u}-2340\frac{M_0^3T^{2+\alpha}}{u}\\
&\quad -4200M_0^3T^{1+\alpha}u;\\
\Delta_T &= -900M_0T^{1+\alpha}-5500M_0^3T^{1+\alpha}\\
&\quad -\frac{10000}{3}M_0^5T^{1+\alpha}+1800M_0^3T^{2+\alpha}-270\frac{M_0^3T^{4+\alpha}}{u^4}\\
&\quad +270\frac{M_0^2T^{3+\alpha}}{u^3}+450\frac{M_0^4T^{3+\alpha}}{u^3}-3600\frac{M_0^3T^{2+\alpha}}{u^2}\\
&\quad -1200\frac{M_0^5T^{2+\alpha}}{u^2}+2610\frac{M_0^3T^{3+\alpha}}{u^2}+2250\frac{M_0^2T^{1+\alpha}}{u}\\
&\quad +4500\frac{M_0^4T^{1+\alpha}}{u}+1250\frac{M_0^6T^{1+\alpha}}{u}-810\frac{M_0^2T^{2+\alpha}}{u}\\
&\quad -1350\frac{M_0^4T^{2+\alpha}}{u}+1750M_0^2T^{1+\alpha}u\\
&\quad +\frac{8750}{3}M_0^4T^{1+\alpha}u-\frac{2500}{3}M_0^3T^{1+\alpha}u^2.
\end{aligned}$$

Although these expressions look quite cumbersome, it can be checked that the upstream equilibrium $(u_0,T_0)=(M_0,1)$ and the downstream equilibrium (u_1,T_1), determined by (5.12), are the stationary points of (6.8): $F_{\mathrm{H}}(u_0,T_0,M_0)=F_{\mathrm{H}}(u_1,T_1,M_0)=0$, $G_{\mathrm{H}}(u_0,T_0,M_0)=G_{\mathrm{H}}(u_1,T_1,M_0)=0$.

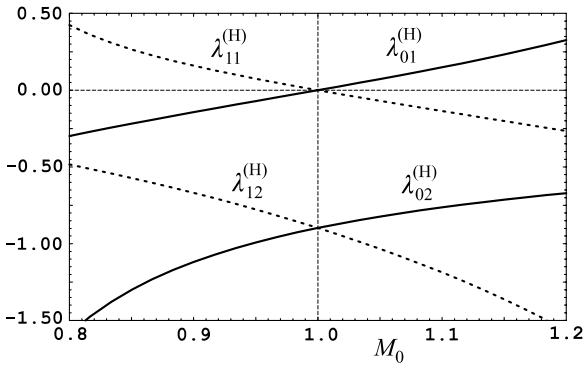

Figure 5. Graphs of the eigenvalues in 13 moments model ($\alpha = 1$).

6.2. Stability analysis of equilibrium points

As in the NSF model, stability analysis of stationary points will show that the critical value of Mach number is $M_0 = 1$ again, meaning that in its neighbourhood one of the eigenvalues determined from linearized equations changes the sign. The intricate character of this result comes from the fact that the critical value of M_0 is related to the highest characteristic speed of Euler's equations (2.2), rather than to any characteristic speed of the hyperbolic system (2.16). However, it is not surprising since the stationary points of (6.8) correspond to the equilibrium manifold of the 13 moments equations (2.16).

Theorem 6.1. *Let $\lambda_{0j}^{(H)}(M_0)$ and $\lambda_{1j}^{(H)}(M_0)$, $j = 1, 2$, denote the eigenvalues of the linearized system derived from (5.11) at the stationary points (u_0, T_0) and (u_1, T_1), respectively. There exists a neighbourhood of the critical value of the parameter $M_0 = 1$ such that one of the eigenvalues changes its sign. Precisely, the following inequalities hold*

$$\begin{aligned} &\lambda_{02}^{(H)}(M_0) < \lambda_{01}^{(H)}(M_0) < 0 \qquad \text{for } M_0 < 1; \\ &\lambda_{02}^{(H)}(M_0) < 0 < \lambda_{01}^{(H)}(M_0) \qquad \text{for } M_0 > 1; \end{aligned} \tag{6.10}$$

$$\begin{aligned} &\lambda_{12}^{(H)}(M_0) < 0 < \lambda_{11}^{(H)}(M_0) \qquad \text{for } M_0 < 1; \\ &\lambda_{12}^{(H)}(M_0) < \lambda_{11}^{(H)}(M_0) < 0 \qquad \text{for } M_0 > 1. \end{aligned} \tag{6.11}$$

The proof of the theorem is given in appendix A. Figure 5 shows graphs of the eigenvalues considered in stability analysis in the case $\alpha = 1$ and illustrates inequalities (6.10) and (6.11). It also helps to conclude that (u_0, T_0) is a stable node in the subsonic case and a saddle point in the supersonic case, whereas (u_1, T_1) is a saddle point in the subsonic case and a stable node in the supersonic case.

Comparison of the results of theorems 6.1 and 5.1 yields that the character of stationary points is different in the NSF model and extended thermodynamics. This property has already been pointed out by Grad [15]. However, the critical eigenvalues behave in the same manner: $\lambda_{01}^{(P)}(M_0)$ and $\lambda_{01}^{(H)}(M_0)$ are strictly increasing functions crossing 0 at $M_0 = 1$, whereas $\lambda_{11}^{(P)}(M_0)$ and $\lambda_{11}^{(H)}(M_0)$ are strictly decreasing functions crossing 0 at the same point.

Phase portraits of dynamical system (6.8) obtained by numerical simulation are shown in figure 6 in the subsonic ($M_0 = 0.8$) and supersonic ($M_0 = 1.2$) cases. The character of the stationary points, indicated by linear stability analysis, is confirmed by these graphs. The solid black lines indicate the heteroclinic orbits connecting stationary points.

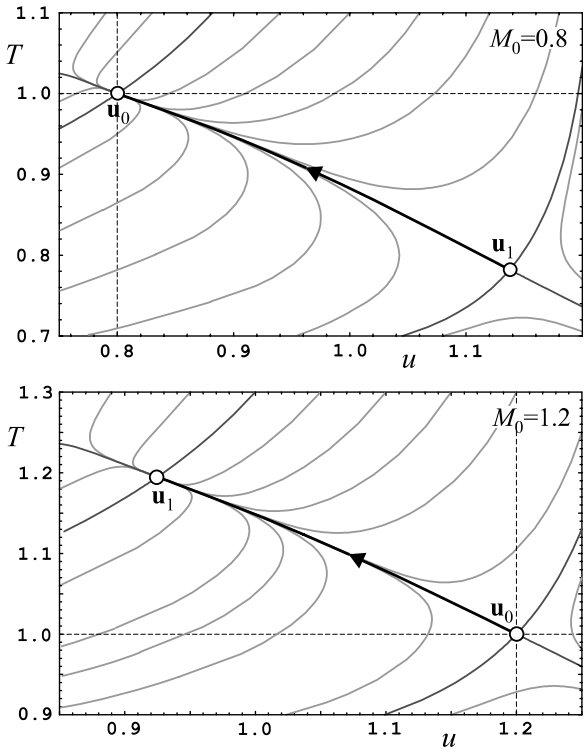

Figure 6. Phase portraits in 13 moments model in subsonic ($M_0 = 0.8$) and supersonic ($M_0 = 1.2$) cases. Heteroclinic orbits indicated by a solid black line.

6.3. Local bifurcation analysis

As in section 5, bifurcation analysis will reveal a transcritical bifurcation pattern in the neighbourhood of the critical value of the bifurcation parameter $M_0 = 1$. Moreover, the bifurcation equation will have the same form as (5.24), up to the second order terms. The results will be presented in the same three steps: transformation to normal form (lemma 6.1), approximation of the centre manifold (lemma 6.2) and derivation of the bifurcation equation (theorem 6.2).

Let Δu and ΔT denote perturbations of equilibrium values (6.6) of u and T and let $\Delta M_0 = M_0 - 1$. With $u = 1 + \Delta M_0 + \Delta u$, $T = 1 + \Delta T$ system (6.8) can be written in suspended form

$$\begin{aligned} \frac{\mathrm{d}\Delta u}{\mathrm{d}\xi} &= F_{\mathrm{H}}(1 + \Delta M_0 + \Delta u, 1 + \Delta T); \\ \frac{\mathrm{d}\Delta T}{\mathrm{d}\xi} &= G_{\mathrm{H}}(1 + \Delta M_0 + \Delta u, 1 + \Delta T); \\ \frac{\mathrm{d}\Delta M_0}{\mathrm{d}\xi} &= 0. \end{aligned} \tag{6.12}$$

Linearization of (6.12) at $(\Delta u, \Delta T, \Delta M_0) = (0, 0, \Delta M_0)$ reads

$$\hat{\boldsymbol{A}}_{\mathrm{H}0}(\Delta M_0) = \begin{pmatrix} \boldsymbol{A}_{\mathrm{H}0}(1 + \Delta M_0) & \mathbf{0} \\ \mathbf{0} & 0 \end{pmatrix}, \tag{6.13}$$

and

$$\hat{\boldsymbol{A}}_{\mathrm{H}0}(0) = \begin{pmatrix} -4/13 & -6/13 & 0 \\ -46/117 & -23/39 & 0 \\ 0 & 0 & 0 \end{pmatrix}. \tag{6.14}$$

Lemma 6.1. *By means of linear transformation*

$$(\Delta u, \Delta T, \Delta M_0) = (-\tfrac{3}{2}y + \tfrac{18}{23}z, y + z, \epsilon) \tag{6.15}$$

system (6.12) is transformed into normal form

$$\begin{aligned} \frac{\mathrm{d}}{\mathrm{d}\xi}\begin{pmatrix} y \\ z \\ \epsilon \end{pmatrix} &= \begin{pmatrix} f_{\mathrm{H}}(y, z, \epsilon) \\ g_{\mathrm{H}}(y, z, \epsilon) \\ 0 \end{pmatrix} \\ &= \boldsymbol{B}_{\mathrm{H}0}(\epsilon)\begin{pmatrix} y \\ z \\ \epsilon \end{pmatrix} + \begin{pmatrix} Y_{\mathrm{H}}(y, z, \epsilon) \\ Z_{\mathrm{H}}(y, z, \epsilon) \\ 0 \end{pmatrix}, \end{aligned} \tag{6.16}$$

where

$$\boldsymbol{B}_{\mathrm{H}0}(0) = \begin{pmatrix} 0 & 0 & 0 \\ 0 & -35/39 & 0 \\ 0 & 0 & 0 \end{pmatrix}, \tag{6.17}$$

and $Y_{\mathrm{H}}(y, z, \epsilon)$ and $Z_{\mathrm{H}}(y, z, \epsilon)$ are at least of the second order in y and z.

The proof of the lemma is given in appendix A. Linearization of (6.16) has double zero eigenvalue at the origin and its centre subspace E^{c} is spanned by $\boldsymbol{e}_{\mathrm{H}1}$ and $\boldsymbol{e}_{\mathrm{H}3}$. Consequently, centre manifold W^{c} has the same general form (5.21) as in the NSF model and has to satisfy the equation

$$\frac{\partial h(y, \epsilon)}{\partial y} f_{\mathrm{H}}(y, h(y, \epsilon), \epsilon) - g_{\mathrm{H}}(y, h(y, \epsilon), \epsilon) = 0. \tag{6.18}$$

Following the arguments of section 3, $h(y, \epsilon)$ will be approximated by a Taylor series expansion in the neighbourhood of the origin. Using second order approximation $h(y, \epsilon) \approx c_{yy}y^2 + c_{y\epsilon}y\epsilon + c_{\epsilon\epsilon}\epsilon^2$ one directly obtains the following result.

Lemma 6.2. *Centre manifold $z = h(y, \epsilon)$ which satisfies equation (6.18) can be approximated by*

$$h(y, \epsilon) \approx \tfrac{184}{245}\epsilon y - \tfrac{115}{196}y^2 \tag{6.19}$$

in the neighbourhood of the origin.

The bifurcation equation for this problem is obtained by inserting (6.19) into $\mathrm{d}y/\mathrm{d}\xi = f_{\mathrm{H}}(y, h(y, \epsilon), \epsilon)$. Taylor series expansion leads to the main result of the analysis.

Theorem 6.2. *Bifurcation of equilibrium $(y, z, \epsilon) = (0, 0, \epsilon)$ of (6.16) appears for the bifurcation value of parameter $\epsilon = 0$ and the corresponding bifurcation equation has the form*

$$\frac{\mathrm{d}y}{\mathrm{d}\xi} = \frac{10}{7}\epsilon y - \frac{20}{7}y^2 + O_3 \tag{6.20}$$

where O_3 denotes terms which vanish along with their first and second derivatives with respect to y and ϵ for $(y, \epsilon) = (0, 0)$.

As was pointed out at the beginning of the section, the bifurcation equation (6.20) for the shock structure problem of the hyperbolic dissipative model has the same form as (5.24) for the parabolic model and the qualitative structure of the bifurcation diagram is completely the same. In such a way, the stable branch of the bifurcating solution $y_1(\epsilon)$ again corresponds to solutions of Rankine–Hugoniot equations (4.1) which are physically admissible in the sense of Lax, and stability considerations of theorem 6.1 play an equivalent role in the dissipative system as Lax's condition play in Euler's model.

A brief résumé is in order, concerned with the results of the last two sections. It was shown, by direct calculation, that two mathematically different dissipative continuum models of gas dynamics have two common features in the context of stability and bifurcation analysis of equilibrium states:

(i) the upstream equilibrium state 'loses' its stability when the shock speed crosses the critical value—the highest characteristic speed (speed of sound) of the equilibrium system; actually, one of the eigenvalues changes its sign in the neighbourhood of $M_0 = 1$;
(ii) the downstream equilibrium state can be regarded as a bifurcating solution and the bifurcation equation reveals a transcritical bifurcation pattern.

Since Lax's condition has not been exploited in this analysis, it was claimed that the stability results of theorems 5.1 and 6.1 provide an equivalent selection rule, at least in these cases, which could be directly applied to dissipative models.

A natural question may be posed about possible generalizations. At this moment it could only be conjectured that these results are valid for general parabolic and hyperbolic dissipative models under certain assumptions, explicitly or implicitly stated in this study. These assumptions are the following:

(i) the shock structure problem is analysed for the shock waves which correspond to the highest characteristic speeds of the equilibrium system; these characteristic speeds are assumed to be genuinely nonlinear;
(ii) dissipative continuum models, either parabolic or hyperbolic, are reduced to the equilibrium one when dissipation is neglected;
(iii) dissipative models considered in this study are compatible with appropriate companion balance laws, i.e. entropy inequalities with convex entropy (this is how the closure problem is resolved in extended thermodynamics [22]);
(iv) the hyperbolic dissipative model can be reduced to a parabolic one through asymptotic expansion akin to the Chapman–Enskog one.

Rigorous study of the stability criterion conjecture has yet to be done. If successful, it will also remove possible redundancy of the above-mentioned assumptions.

7. Further application of bifurcation analysis

In the absence of general results, capability of stability and bifurcation analysis for further application can be tested on other systems. It will be shown in this section that analysis yields the same results in more involved models as long as they can be reduced to the same equilibrium system of Euler's equations. Particular examples of the 14 and 21 moments equations of extended thermodynamics will be analysed. A comment will also be given about the linear stability analysis in the neighbourhood of the other critical values of the bifurcation parameter. An interesting possibility for construction of approximate solutions, based upon the solution of the bifurcation equation in the neighbourhood of the critical point, will also be shown. Discussion will be closed by indication of the benefits of stability analysis in numerical calculation of shock structure.

7.1. Extended thermodynamics with 14 and 21 fields

In addition to nonequilibrium fields of stress σ and heat flux q, extended thermodynamics with 14 fields introduce another variable Θ—the nonequilibrium part of the fourth moment of the distribution function [17]. This results in additional balance law which have to be adjoined to (2.16). Using (6.7) the sock structure equations can be reduced to a set of three ODEs, with u, T and Θ as unknown fields.

By applying the same procedure of stability and bifurcation analysis as in sections 5 and 6, analogous results are obtained. In particular, there exists a neighbourhood of the critical value of the parameter $M_0 = 1$ such that one of the eigenvalues changes sign

$$\begin{aligned} &\lambda_{03}^{(14)}(M_0) < \lambda_{02}^{(14)}(M_0) < \lambda_{01}^{(14)}(M_0) < 0 \qquad \text{for } M_0 < 1; \\ &\lambda_{03}^{(14)}(M_0) < \lambda_{02}^{(14)}(M_0) < 0 < \lambda_{01}^{(14)}(M_0) \qquad \text{for } M_0 > 1; \end{aligned} \tag{7.1}$$

$$\begin{aligned} &\lambda_{13}^{(14)}(M_0) < \lambda_{12}^{(14)}(M_0) < 0 < \lambda_{11}^{(14)}(M_0) \qquad \text{for } M_0 < 1; \\ &\lambda_{13}^{(14)}(M_0) < \lambda_{12}^{(14)}(M_0) < \lambda_{11}^{(14)}(M_0) < 0 \qquad \text{for } M_0 > 1. \end{aligned} \tag{7.2}$$

To be precise,

$$\begin{aligned} &\lambda_{01}^{(14)}(1) = 0; \qquad \frac{\mathrm{d}\lambda_{01}^{(14)}(1)}{\mathrm{d}M_0} = \frac{10}{7}; \\ &\lambda_{11}^{(14)}(1) = 0; \qquad \frac{\mathrm{d}\lambda_{11}^{(14)}(1)}{\mathrm{d}M_0} = -\frac{10}{7}; \end{aligned} \tag{7.3}$$

The suspended system of equations in normal form, obtained via linear transformation $(\Delta u, \Delta T, \Delta\Theta, \Delta M_0) \to (y, z_1, z_2, \epsilon)$, has two-dimensional centre manifold approximately, while the bifurcation equation has the same form as (5.24) and (6.20) as in the NSF and 13 moments case.

The 21 moments equations do not provide any substantially new contribution whatsoever (for the model consult [22]). Although the order of the shock structure ODE system is greater by one, a single eigenvalue again plays a distinguished role leading to the same bifurcation pattern. Therefore, even in more involved problems stability and bifurcation analysis supports our conjecture about two common properties of dissipative models, given at the end of previous section, as long as the full system of governing equations has the Euler's system (2.2) as an equilibrium system.

A note has to be added about the stability analysis. In procedures applied in this study, the order of the original shock structure system has always been immediately reduced by means of conservation laws (for example, see equation (6.7) derived from the first three equations of (6.5)). As a consequence, all the eigenvalues were real and different from zero except in the critical case $M_0 = 1$. What would have happened if this reduction had not been done? In this case there will appear multiple zero eigenvalue whose algebraic multiplicity is equal to the number of conservation laws. However, this fact does not affect the structure and behaviour of other eigenvalues and the main conclusions of stability analysis will remain the same.

7.2. Other critical values of the bifurcation parameter

The main issue of this study was stability and bifurcation analysis of the shock structure problem. It naturally arises in the neighbourhood of the critical value of the shock speed which corresponds to the highest genuinely nonlinear characteristic speed of the equilibrium system. However, there remains an open question about solution behaviour in the neighbourhood of other critical values of the shock speed corresponding to genuinely nonlinear characteristic

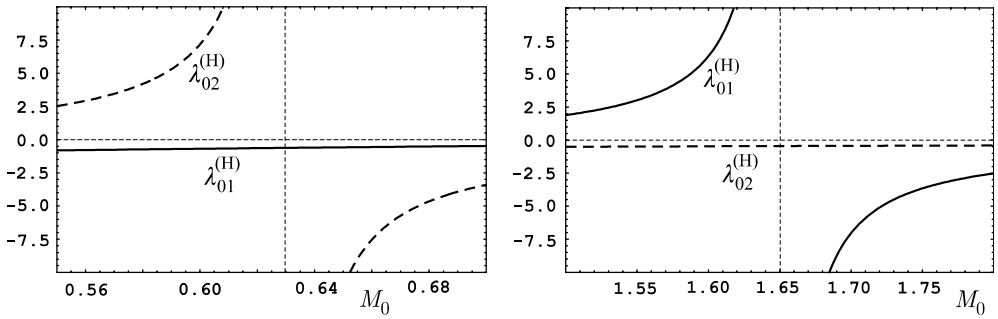

Figure 7. Eigenvalues in the neighbourhood of upstream singular points (7.4).

speeds of the hyperbolic dissipative systems. This problem will be outlined for the 13 moments model (6.8).

Having in mind the structure of equations (6.9) which describe the shock profile, one may ask, when will the right-hand sides become singular, i.e. $\Delta = 0$. By simple calculation it can be shown that the singularity condition is satisfied for

$$M_0 = \pm 0.6297; \qquad M_0 = \pm 1.6503. \tag{7.4}$$

These solutions correspond to characteristic speeds (2.18) of the 13 moments model (2.16). Weiss [30] analysed singular points in detail in the shock structure problem for extended thermodynamic models and showed that the continuous shock structure ceases to exist when M_0 becomes greater than the highest critical value. This important fact was pointed out by Grad [15] in the case of the 13 moments equations. A general result of this kind, valid for hyperbolic systems of balance laws with convex extension, has been proven by Boillat and Ruggeri [3].

Our analysis will be restricted to calculation of the eigenvalues of the linearized system at the equilibrium state in the neighbourhood of the critical values (7.4). Let us recall that $\lambda_{01}^{(H)}(M_0)$ and $\lambda_{11}^{(H)}(M_0)$ change the sign in the neighbourhood of $M_0 = 1$. For the upstream equilibrium (figure 7), $\lambda_{01}^{(H)}(M_0)$ is monotonically increasing in the neighbourhood of $M_0 = 0.6297$, while $\lambda_{02}^{(H)}(M_0)$ is singular at the same point, having vertical asymptotes. On the other hand, $\lambda_{01}^{(H)}(M_0)$ becomes singular at $M_0 = 1.6503$ with vertical asymptotes, while $\lambda_{02}^{(H)}(M_0)$ is monotonically increasing in its neighbourhood.

For downstream equilibrium behaviour is a bit different. Singularities of eigenvalues are not related to critical values (7.4), but rather to

$$M_0 = \pm 0.6735; \qquad M_0 = \pm 1.85905. \tag{7.5}$$

Moreover, in the neighbourhood of these points both eigenvalues have one-sided vertical asymptotes (figure 8). In particular, in the neighbourhood of $M_0 = 0.6735$ eigenvalue $\lambda_{11}^{(H)}(M_0)$ is finite from the left, but increases to ∞ from the right. At the same time $\lambda_{12}^{(H)}(M_0)$ is finite from the right while it tends to $-\infty$ from the left. In the neighbourhood of $M_0 = 1.859\,05$ the behaviour of eigenvalues from the left and from the right is completely the same as in the previous case.

The appearance of singularities of the eigenvalues in the neighbourhood of (7.4) and (7.5) can be related to the well-known subshock problem. Apart from already mentioned papers, a very instructive example of the subshock appearance has been given by Torrilhon [28]. Moreover, recently reported results by Currò and Fusco [9] showed that for $1.6503 < M_0 < 1.859\,05$ there exists a discontinuous travelling shock structure

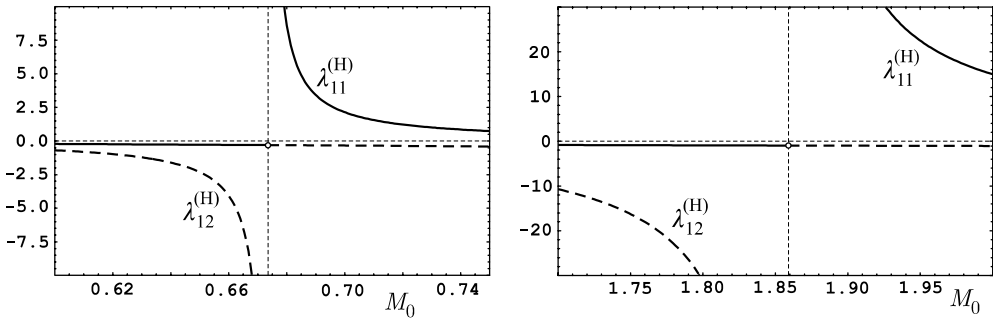

Figure 8. Eigenvalues in the neighbourhood of downstream singular points (7.5).

with a single jump discontinuity. It is shown to be a consequence of the fact that equilibrium states in phase space lie on different sides of the so-called singular barrier. When $M_0 > 1.859\,05$ a discontinuous shock structure is observed with two jump discontinuities. These discontinuities were governed by Rankine–Hugoniot equations for the differential part of the full hyperbolic system of 13 moments equations. A possible way out of this problem has been given by Au, Torrilhon and Weiss [1] through higher order moment systems of extended thermodynamics. Although some particular conclusions could be drawn from this analysis, a careful study of the singularities is needed in order to reveal all the implications of their existence.

7.3. Approximate solutions for very weak shocks

The main intention of this study was to point out the common features of two different dissipative models which could be drawn from stability and bifurcation analysis. Its terminal points, i.e. bifurcation equations (5.24) and (6.20), can serve as a starting point for the construction of approximate analytical solutions of the shock structure problem. Namely, when O_3 terms are neglected, an explicit solution of bifurcation equations can be derived

$$y(\xi) = \frac{\epsilon}{2} f(\epsilon, \xi); \qquad f(\epsilon, \xi) = \mathrm{e}^{\frac{10}{7}\epsilon\xi}(1 + \mathrm{e}^{\frac{10}{7}\epsilon\xi})^{-1}, \tag{7.6}$$

where the initial condition $y(0) = \epsilon/4$ was used for convenience in positioning the shock profile in the moving reference frame. In the case of the parabolic NSF model, the approximate solution for the centre manifold (5.23) used in conjunction with (7.6) yields an approximate solution for $z(\xi)$, while the linear transformation (5.18) leads to approximate solutions for perturbations $\Delta u(\xi)$ and $\Delta T(\xi)$. Finally, using the relations $u = 1 + \Delta M_0 + \Delta u$, $T = 1 + \Delta T$ and $M_0 = 1 + \Delta M_0$, the approximate solutions for the shock profile are obtained

$$\begin{aligned} u_P(\xi) &= M_0 - \tfrac{3}{4}(M_0 - 1) f(M_0 - 1, \xi) \\ &\quad + \tfrac{9}{8}(M_0 - 1)^2 (\tfrac{16}{49} f(M_0 - 1, \xi) - \tfrac{25}{196} f(M_0 - 1, \xi)^2); \end{aligned} \tag{7.7}$$

$$\begin{aligned} T_P(\xi) &= 1 + \tfrac{1}{2}(M_0 - 1) f(M_0 - 1, \xi) \\ &\quad + (M_0 - 1)^2 (\tfrac{16}{49} f(M_0 - 1, \xi) - \tfrac{25}{196} f(M_0 - 1, \xi)^2). \end{aligned} \tag{7.8}$$

An approximate solution for the shock structure in the case of the hyperbolic 13 moments model can be constructed in the same manner. From the approximate solution for the centre manifold (6.19) and (7.6) approximate $z(\xi)$ is derived. Using linear transformation (6.15) and

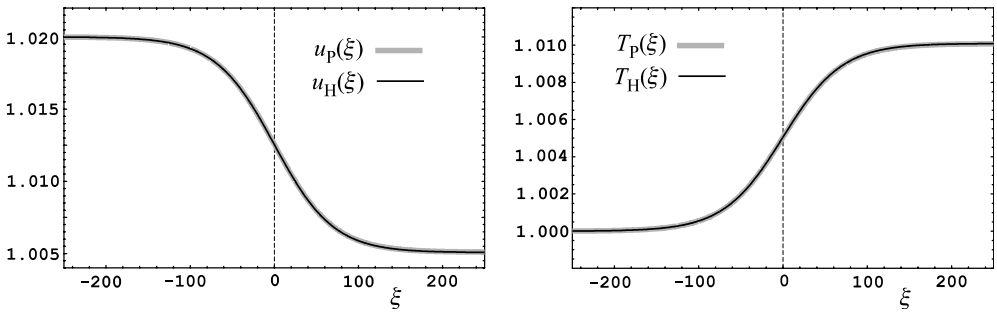

Figure 9. Approximate analytical solutions of the shock structure equations for $M_0 = 1.02$.

expressions for u, T and M_0 in terms of perturbations, the following approximate solutions for the shock profile are obtained

$$u_H(\xi) = M_0 - \tfrac{3}{4}(M_0 - 1) f(M_0 - 1, \xi) + \tfrac{18}{23}(M_0 - 1)^2 (\tfrac{92}{245} f(M_0 - 1, \xi) - \tfrac{115}{784} f(M_0 - 1, \xi)^2); \tag{7.9}$$

$$T_H(\xi) = 1 + \tfrac{1}{2}(M_0 - 1) f(M_0 - 1, \xi) + (M_0 - 1)^2 (\tfrac{92}{245} f(M_0 - 1, \xi) - \tfrac{115}{784} f(M_0 - 1, \xi)^2). \tag{7.10}$$

It is important to note that solutions (7.7)–(7.10) are reliable for very weak shocks only ($\Delta M_0 \approx 10^{-2}$). If stronger shocks are calculated using these equations, discrepancies will occur between the values of u and T for $\xi \to \infty$ and their downstream equilibrium values (5.12) derived from Rankine–Hugoniot equations. Figure 9 shows the graphs of approximate analytical solutions (7.7)–(7.10) calculated for $M_0 = 1.02$. Although they have different analytical forms, their graphs are almost indistinguishable, which is a consequence of the weak shock approximation they are restricted to, and the fact that the difference between (7.7)–(7.8) and (7.9)–(7.10) is of the order $O(\Delta M_0^2)$. This approximation also dictates the necessity of a rather wide domain of the independent variable in order to capture the whole profile of the weak shock.

7.4. Numerical aspects of stability analysis

Phase portraits and shock structure solutions in sections 5 and 6 were calculated numerically. In the case of the second order system it is quite common to determine the heteroclinic orbit by solving the shock structure equations numerically as an initial value problem [13]. However, an increase in the order of the system also increases the difficulties. Therefore, the shock structure problems of order higher than two were usually solved as boundary value problems by means of the finite-difference method [29].

Results presented in this paper within stability analysis provide a tool for numerical calculation of the shock profile as the initial value problem. Actually, since the critical eigenvalue is determined as the one which changes the sign, one may calculate corresponding eigenvectors in upstream and downstream equilibria and in this way determine the asymptotic behaviour of the shock profile. Moreover, in the case of hyperbolic dissipative models, eigenvector $\boldsymbol{e}_{01}$ corresponding to the critical eigenvalue λ_{01}, evaluated at the upstream equilibrium $\boldsymbol{u}_0$, can be used to determine the initial values of the state variables for calculation of the shock structure, $\boldsymbol{u}_{\text{init}} = \boldsymbol{u}_0 + \delta \boldsymbol{e}_{01}$, for appropriately chosen small real number δ. Since state variables in the shock structure problem converge rapidly to the equilibrium values, calculation may be performed on a finite computational domain. A similar asymptotic technique has been

devised by Beyn [6] in the boundary value problem of heteroclinic orbits and its truncation from an infinite domain to a finite one. However, these optimistic ideas have to be carefully tested. Weiss [30] claimed that the appearance of regular singular points within the profile may prevent simple calculation of the shock profile using the initial value procedure. Detailed analysis of numerical aspects is beyond the scope of this study and will be the topic of prospective work.

8. Conclusions

The shock structure problem in continuum theory of fluids is a well-known and challenging problem, both physically and mathematically. In the latter context two different types of mathematical models appeared with the intention of describing this phenomenon in the appropriate way, i.e. taking into account dissipative mechanisms. The first type—parabolic systems of PDEs—is usually identified with, but not exhausted by, the NSF model which introduces dissipation in the classical Euler's equations of gas dynamics through diffusive terms, related to viscosity and heat conduction. Another group of models falls into the category of hyperbolic systems of balance laws with dissipative source terms. The 13 moments model, obtained in the context of extended thermodynamics, has been taken as a paradigmatic one for this group. This paper tends to impart the common ground of these models through stability and bifurcation analysis of equilibrium states.

The analysis was based upon the ODE system of the shock structure equations derived from the original PDE model using travelling wave ansatz. In such a way the equilibrium states became stationary points of the dynamical system describing the shock structure. The first important result of the study is obtained by means of linear stability analysis. It was demonstrated that in both models there always exists a distinguished eigenvalue which changes the sign in the neighbourhood of the critical value of the parameter $M_0 = 1$, corresponding to the highest characteristic speed of the equilibrium system—Euler's model. Since Lax's admissibility condition has not been used in the analysis, stability results stated in theorems 5.1 and 6.1 can be used as selection rules for admissible shock structures in dissipative models. Bifurcation analysis gave the second result by revealing the common transcritical bifurcation pattern which appears in both models (theorems 5.2 and 6.2).

This study opened some new questions indicated in section 7. First, it is natural to seek for possible generalizations of the results presented here. For what concerns parabolic models, it seems that a positive answer could be given in a straightforward manner, whereas for hyperbolic systems of balance laws thorough study has yet to be performed. Second, a rigorous singularity analysis in hyperbolic models, related to other critical values of the parameter, is another open question. Finally, the computational aspect of stability analysis and its consequences in analytical and numerical calculation of the shock profiles has to be carefully studied. These are possible lines of investigation in future work.

Acknowledgments

This work was supported by the Ministry of Science of the Republic of Serbia within the project 'Contemporary problems of mechanics of deformable bodies' (Project No 144019). The author is indebted to Professor Tommaso Ruggeri (University of Bologna, Italy) and Professor Ingo Müller (Technical University Berlin, Germany) for numerous fruitful discussions and useful comments and suggestions during the preparation of this paper.

Appendix A. Proofs of theorems and lemmas

Proof of theorem 5.1. The proof will be given for the upstream equilibrium state first and then for the downstream equilibrium. The Jacobian matrix for system (5.11) at $(u_0, T_0) = (M_0, 1)$ reads

$$\boldsymbol{A}_{\mathrm{P}0}(M_0) = \begin{pmatrix} \frac{1}{4}(5M_0 - \frac{3}{M_0}) & \frac{3}{4} \\ \frac{4}{9} & \frac{2}{3}M_0 \end{pmatrix}, \tag{A.1}$$

while corresponding eigenvalues are

$$\begin{gathered} \lambda_{01}^{(\mathrm{P})}(M_0) = \frac{D_{0-}}{24M_0}; \qquad \lambda_{02}^{(\mathrm{P})}(M_0) = \frac{D_{0+}}{24M_0}; \\ D_{0\mp} = -9 + 23M_0^2 \mp \sqrt{81 + 66M_0^2 + 49M_0^4}, \end{gathered} \tag{A.2}$$

and the following holds

$$\begin{gathered} \lambda_{01}^{(\mathrm{P})}(1) = 0; \qquad \lambda_{02}^{(\mathrm{P})}(1) = \tfrac{7}{6}; \\ \frac{\mathrm{d}\lambda_{01}^{(\mathrm{P})}(1)}{\mathrm{d}M_0} = \frac{10}{7}. \end{gathered} \tag{A.3}$$

By the continuity argument it follows that there is a neighbourhood of $M_0 = 1$ in which $\lambda_{01}^{(\mathrm{P})}(M_0) < 0$ for $M_0 < 1$ and $\lambda_{01}^{(\mathrm{P})}(M_0) > 0$ for $M_0 > 1$, while $\lambda_{02}^{(\mathrm{P})}(M_0) > 0$ in either case which proves (5.13).

The Jacobian matrix at (u_1, T_1) given by (5.12) reads

$$\begin{aligned} \boldsymbol{A}_{\mathrm{P}1}(M_0) = {} & 16^{\alpha}\left(14 - \frac{3}{M_0^2} + 5M_0^2\right)^{-\alpha} \\ & \times \begin{pmatrix} \dfrac{9M_0 - 5M_0^3}{2(3 + M_0^2)} & \dfrac{3M_0^2}{3 + M_0^2} \\ \dfrac{1}{9}\left(-1 + 5M_0^2\right) & \dfrac{2}{3}M_0 \end{pmatrix}, \end{aligned} \tag{A.4}$$

while the corresponding eigenvalues are

$$\begin{aligned} \lambda_{11}^{(\mathrm{P})}(M_0) &= \frac{16^{\alpha}\left(14 - \dfrac{3}{M_0^2} + 5M_0^2\right)^{-\alpha}}{12(3 + M_0^2)} D_{1-} \\ \lambda_{12}^{(\mathrm{P})}(M_0) &= \frac{16^{\alpha}\left(14 - \dfrac{3}{M_0^2} + 5M_0^2\right)^{-\alpha}}{12(3 + M_0^2)} D_{1+}; \\ D_{1\mp} &= 39 - 11M_0^2 \mp \sqrt{81 + 102M_0^2 + 601M_0^4} \end{aligned} \tag{A.5}$$

and the following holds

$$\begin{gathered} \lambda_{11}^{(\mathrm{P})}(1) = 0; \qquad \lambda_{12}^{(\mathrm{P})}(1) = \frac{7}{6}; \\ \frac{\mathrm{d}\lambda_{11}^{(\mathrm{P})}(1)}{\mathrm{d}M_0} = -\frac{10}{7}. \end{gathered} \tag{A.6}$$

Again, the continuity argument helps to conclude that there is a neighbourhood of $M_0 = 1$ in which $\lambda_{11}^{(\mathrm{P})}(M_0) > 0$ for $M_0 < 1$ and $\lambda_{11}^{(\mathrm{P})}(M_0) < 0$ for $M_0 > 1$, while $\lambda_{12}^{(\mathrm{P})}(M_0) > 0$ in either case, which proves (5.14).

Note that at (u_0, T_0) eigenvalues depend only on M_0 and not on α, while at (u_1, T_1) they also depend on the type of gas through α. However, their values as well as behaviour of the critical eigenvalue at $M_0 = 1$ are independent of α.

Proof of lemma 5.1. By straightforward calculation from (5.17) one can obtain the eigenvalues of $\hat{\boldsymbol{A}}_{\mathrm{P0}}(0)$, $(\lambda_{\mathrm{P1}}, \lambda_{\mathrm{P2}}, \lambda_{\mathrm{P3}}) = (0, 7/6, 0)$, and the corresponding set of eigenvectors $(\boldsymbol{e}_{\mathrm{P1}}, \boldsymbol{e}_{\mathrm{P2}}, \boldsymbol{e}_{\mathrm{P3}})$ which actually determines the transformation matrix

$$\boldsymbol{T}_{\mathrm{P}} = (\boldsymbol{e}_{\mathrm{P1}}, \boldsymbol{e}_{\mathrm{P2}}, \boldsymbol{e}_{\mathrm{P3}}) = \begin{pmatrix} -3/2 & 9/8 & 0 \\ 1 & 1 & 0 \\ 0 & 0 & 1 \end{pmatrix}. \tag{A.7}$$

Linear transformation (5.18) is obtained through $(\Delta u, \Delta T, \Delta M_0)^{\mathrm{T}} = \boldsymbol{T}_{\mathrm{P}} \cdot (y, z, \epsilon)^{\mathrm{T}}$, where superposed T stands for transposition. The right-hand side of (5.19) is determined as $(f_{\mathrm{P}}(y, z, \epsilon), g_{\mathrm{P}}(y, z, \epsilon), 0)^{\mathrm{T}} = \boldsymbol{T}_{\mathrm{P}}^{-1} \cdot (\hat{F}_{\mathrm{P}}(y, z, \epsilon), \hat{G}_{\mathrm{P}}(y, z, \epsilon), 0)^{\mathrm{T}}$, where $\hat{F}_{\mathrm{P}}$ and $\hat{G}_{\mathrm{P}}$ are obtained from F_{P} and G_{P} when $(\Delta u, \Delta T, \Delta M_0)$ is substituted by means of (5.18). The linear part $\boldsymbol{B}_{\mathrm{P0}}(\epsilon)$ can be obtained either as a Jacobian of the right-hand side of the complete system evaluated at $(y, z, \epsilon) = (0, 0, \epsilon)$, or through $\boldsymbol{B}_{\mathrm{P0}}(\epsilon) = \boldsymbol{T}_{\mathrm{P}}^{-1} \cdot \hat{\boldsymbol{A}}_{\mathrm{P0}}(\epsilon) \cdot \boldsymbol{T}_{\mathrm{P}}$. For the sake of brevity complete expressions for f_{P} and g_{P} will be omitted since they can be obtained in a straightforward way.

Proof of theorem 6.1. The Jacobian matrix for system (6.8) at $(u_0, T_0) = (M_0, 1)$ reads

$$\begin{aligned} \boldsymbol{A}_{\mathrm{H0}}(M_0) &= \frac{1}{27 - 78M_0^2 + 25M_0^4} \\ &\times \begin{pmatrix} \dfrac{-9 + 42M_0^2 - 25M_0^4}{M_0} & 3(3 + M_0^2) \\ \dfrac{54 - 162M_0^2 + 200M_0^4}{9M_0^2} & \dfrac{-18 + 114M_0^2 - 50M_0^4}{3M_0} \end{pmatrix}, \end{aligned} \tag{A.8}$$

while corresponding eigenvalues are

$$\begin{aligned} \lambda_{01}^{(\mathrm{H})}(M_0) &= \frac{5D_{0-}}{6M_0(27 - 78M_0^2 + 25M_0^4)}; \\ \lambda_{02}^{(\mathrm{H})}(M_0) &= \frac{5D_{0+}}{6M_0(27 - 78M_0^2 + 25M_0^4)}; \\ D_{0\mp} &= -9 + 48M_0^2 - 25M_0^4 \\ &\quad \mp\sqrt{81 - 216M_0^2 + 234M_0^4 + 72M_0^6 + 25M_0^8}, \end{aligned} \tag{A.9}$$

and the following holds

$$\begin{aligned} &\lambda_{01}^{(\mathrm{H})}(1) = 0; \qquad \lambda_{02}^{(\mathrm{H})}(1) = -\frac{35}{39}; \\ &\frac{\mathrm{d}\lambda_{01}^{(\mathrm{H})}(1)}{\mathrm{d}M_0} = \frac{10}{7}. \end{aligned} \tag{A.10}$$

By the continuity argument it follows that there is a neighbourhood of $M_0 = 1$ in which $\lambda_{01}^{(\mathrm{H})}(M_0) < 0$ for $M_0 < 1$ and $\lambda_{01}^{(\mathrm{H})}(M_0) > 0$ for $M_0 > 1$, while $\lambda_{02}^{(\mathrm{H})}(M_0) < 0$ in either case which proves (6.10).

The Jacobian matrix at (u_1, T_1) determined by (5.12) reads

$$\boldsymbol{A}_{\mathrm{H1}}(M_0) = 16^{\alpha}\frac{(1-5M_0^2)\left(14-\dfrac{3}{M_0^2}+5M_0^2\right)^{-\alpha}}{(3+M_0^2)(243-606M_0^2+155M_0^4)} \times \begin{pmatrix} 4M_0(45-66M_0^2+5M_0^4) & -96M_0^4 \\ \frac{1}{18}(585-402M_0^2+185M_0^4) & \frac{1}{3}(405-738M_0^2-35M_0^4) \end{pmatrix}. \tag{A.11}$$

Corresponding eigenvalues $\lambda_{11}^{(\mathrm{H})}(M_0)$ and $\lambda_{12}^{(\mathrm{H})}(M_0)$ can be evaluated explicitly, but have a rather cumbersome form. Nevertheless, the following results can be derived:

$$\lambda_{11}^{(\mathrm{H})}(1) = 0; \qquad \lambda_{12}^{(\mathrm{H})}(1) = -\frac{35}{39}; \qquad \frac{\mathrm{d}\lambda_{11}^{(\mathrm{H})}(1)}{\mathrm{d}M_0} = -\frac{10}{7}, \tag{A.12}$$

which, due to continuity, lead to a conclusion that there is a neighbourhood of $M_0 = 1$ in which $\lambda_{11}^{(\mathrm{H})}(M_0) > 0$ for $M_0 < 1$ and $\lambda_{11}^{(\mathrm{H})}(M_0) < 0$ for $M_0 > 1$, while $\lambda_{12}^{(\mathrm{H})}(M_0) < 0$ in either case, which proves (6.11).

Proof of lemma 6.1. From (6.14) the eigenvalues of $\hat{\boldsymbol{A}}_{\mathrm{H0}}(0)$ are calculated, $(\lambda_{\mathrm{H1}}, \lambda_{\mathrm{H2}}, \lambda_{\mathrm{H3}}) = (0, -35/39, 0)$, along with the corresponding set of eigenvectors $(\boldsymbol{e}_{\mathrm{H1}}, \boldsymbol{e}_{\mathrm{H2}}, \boldsymbol{e}_{\mathrm{H3}})$ which determines the transformation matrix

$$\boldsymbol{T}_{\mathrm{H}} = (\boldsymbol{e}_{\mathrm{H1}}, \boldsymbol{e}_{\mathrm{H2}}, \boldsymbol{e}_{\mathrm{H3}}) = \begin{pmatrix} -3/2 & 18/23 & 0 \\ 1 & 1 & 0 \\ 0 & 0 & 1 \end{pmatrix}. \tag{A.13}$$

Linear transformation (6.15) is determined by $(\Delta u, \Delta T, \Delta M_0)^{\mathrm{T}} = \boldsymbol{T}_{\mathrm{H}} \cdot (y, z, \epsilon)^{\mathrm{T}}$. The right-hand side of (6.16) is determined as $(f_{\mathrm{H}}(y, z, \epsilon), g_{\mathrm{H}}(y, z, \epsilon), 0)^{\mathrm{T}} = \boldsymbol{T}_{\mathrm{H}}^{-1} \cdot (\hat{F}_{\mathrm{H}}(y, z, \epsilon), \hat{G}_{\mathrm{H}}(y, z, \epsilon), 0)^{\mathrm{T}}$, where $\hat{F}_{\mathrm{H}}$ and $\hat{G}_{\mathrm{H}}$ are obtained from F_{H} and G_{H} when $(\Delta u, \Delta T, \Delta M_0)$ is substituted by means of (6.15). The linear part $\boldsymbol{B}_{\mathrm{H0}}(\epsilon)$ can be obtained either as a Jacobian of the right-hand side of the complete system evaluated at $(y, z, \epsilon) = (0, 0, \epsilon)$, or through $\boldsymbol{B}_{\mathrm{H0}}(\epsilon) = \boldsymbol{T}_{\mathrm{H}}^{-1} \cdot \hat{\boldsymbol{A}}_{\mathrm{H0}}(\epsilon) \cdot \boldsymbol{T}_{\mathrm{H}}$. For the sake of brevity complete expressions for f_{H}, g_{H} and $\boldsymbol{B}_{\mathrm{H0}}(\epsilon)$ will be omitted.

References

[1] Au J D, Torrilhon M and Weiss W 2001 The shock tube study in extended thermodynamics *Phys. Fluids* **13** 2423–32

[2] Azevedo A V, Marchesin D, Plohr B and Zumbrun K 1999 Bifurcation of nonclassical viscous shock profiles from the constant state *Commun. Math. Phys.* **202** 267–90

[3] Boillat G and Ruggeri T 1998 On the shock structure problem for hyperbolic system of balance laws and convex entropy *Contin. Mech. Thermodyn.* **10** 285–92

[4] Bose C, Illner R and Ukai S 1998 On shock wave solutions for discrete velocity models of the Boltzmann equation *Transport Theory Statist. Phys.* **27** 35–66

[5] Bernhoff N and Bobylev A 2007 Weak shock waves for the general discrete velocity model of the Boltzmann equation *Commun. Math. Sci.* **5** 815–32

[6] Beyn W-J 1990 The numerical computation of connecting orbits in dynamical systems *IMA J. Numer. Anal.* **10** 379–405

[7] Caflisch R E and Nicolaenko B 1982 Shock profile solutions of the Boltzmann equation *Commun. Math. Phys.* **86** 161–94

[8] Courant R and Friedrichs K O 1948 *Supersonic Flow and Shock Waves* (New York: Interscience Publishers)
[9] Currò C and Fusco D 2005 Discontinuous travelling wave solutions for a class of dissipative hyperbolic models *Rend. Mat. Acc. Lincei* **16** 61–71
[10] Dafermos C M 2005 *Hyperbolic Conservation Laws in Continuum Physics* 2nd edn (Berlin: Springer)
[11] Farjami Y and Hesaaraki M 1998 Structure of shock waves in planar motion of plasma *Nonlinearity* **11** 797–821
[12] Gilbarg D 1951 The existence and limit behavior of the one-dimensional shock layer *Am. J. Math.* **73** 256–74
[13] Gilbarg D and Paolucci D 1953 The structure of shock waves in the continuum theory of fluids *J. Ration. Mech. Anal.* **2** 617–42
[14] Grad H 1949 On the kinetic theory of rarefied gases *Commun. Pure Appl. Math.* **2** 331–407
[15] Grad H 1952 The profile of a steady planar shock wave *Commun. Pure Appl. Math.* **5** 257–300
[16] Guckenheimer J and Holmes P 1986 *Nonlinear Oscillations, Dynamical Systems and Bifurcations of Vector Fields* (New York: Springer)
[17] Kremer G M 1986 Extended thermodynamics of ideal gases with 14 fields *Ann. Inst. H. Poincaré Phys. Théor.* **45** 419–40
[18] Lax P D 1957 Hyperbolic systems of conservation laws: II *Commun. Pure Appl. Math.* **10** 537–66
[19] Lorin E 2003 Existence of viscous profiles for the compressible Navier–Stokes equations *Appl. Anal.* **82** 645–54
[20] Liu T-P 1987 Hyperbolic conservation laws with relaxation *Commun. Math. Phys.* **108** 153–75
[21] Majda A and Pego R L 1985 Stable viscosity matrices for systems of conservation laws *J. Diff. Eqns* **56** 229–62
[22] Müller I and Ruggeri T 1998 *Rational Extended Thermodynamics* (New York: Springer)
[23] Nicolaenko B and Thurber J K 1975 Weak shock and bifurcating solutions of the non-linear Boltzmann equation *J. Mécanique* **14** 305–38
[24] Perko L 2001 *Differential Equations and Dynamical Systems* 3rd edn (New York: Springer)
[25] Schecter S 1992 Heteroclinic bifurcation theory and Riemann problems *Mat. Contemp.* **3** 165–90
[26] Serre D 1999 *Systems of Conservation Laws* (Cambridge: Cambridge University Press)
[27] Simić S S 2008 A note on shock profile in dissipative hyperbolic and parabolic models *Publ. Inst. Math. (N.S.)* **84** 97–107
[28] Torrilhon M 2000 Characteristic waves and dissipation in the 13-moment-case *Contin. Mech. Thermodyn.* **12** 289–301
[29] Torrilhon M and Struchtrup H 2004 Regularized 13-moment equations: shock structure calculations and comparison to Burnett models *J. Fluid Mech.* **513** 171–98
[30] Weiss W 1995 Continuous shock structure in extended thermodynamics *Phys. Rev.* E **52** R5760–3
[31] Yong W-A and Zumbrun K 2000 Existence of relaxation shock profiles for hyperbolic conservation laws *SIAM J. Appl. Math.* **60** 1565–75